# Supplementary Materials for

## Dysregulated methylation–ubiquitination crosstalk accelerates intervertebral disc degeneration via MED12 destabilization and cGAS/STING activation

Huaizhen Liang *et al.*

*Corresponding author. Email: caoyangunion@hust.edu.cn

**This PDF file includes:**

Materials and Methods
Supplemental figure 1 to 10
Supplemental table 1 to 12

## Materials and Methods

### RNA interference and plasmid transfection

For RNA interference, gene-specific small interfering RNAs (siRNAs) targeting PRMT2, FBXO7, MED12, and STING and nontargeting scrambled siRNAs (as negative controls) were transfected into cells using Lipofectamine 2000 (Invitrogen) following the manufacturer's protocol. The cells were harvested 72 hours posttransfection for subsequent analyses. The knockdown efficiency was validated by western blotting. Further information on the siRNA sequences is provided in Supplementary Table 8.

Human FBXO7 wild type (WT), truncated FBXO7 (amino acids 1-324, 325-522, and Δ332-375), FBXO7 mutants (R504K and R504F) and rat MED12 wild type (WT) were separately tagged with GFP and cloned and inserted into the empty vector plasmid pCDNA3.1 to obtain the overexpression plasmids. Human WT PRMT2 and truncated PRMT2 (amino acids 88-433) were separately tagged with HA and cloned and inserted into the empty vector plasmid pCDNA3.1 to obtain the overexpression plasmids. Human WT MED12 and truncated MED12 (amino acids 1-597, 589-964, 959-1728, and 1616-2177) and mutants (K429R, K762R, K785R, K1001R, K1634R, K1643R, K1664R, K1673R, and K1674R) were separately tagged with Flag and cloned and inserted into the empty vector plasmid pCDNA3.1 to obtain the overexpression plasmids. Human ubiquitin WT, K-only (K48-linked and K63-linked) and K-mutated (K48R or K63R) constructs were cloned and inserted into the empty vector plasmid pmCherry-HA-6×His. For efficient transient transfection, NP cells and HEK293T cells were transfected with the previously described plasmids using Lipofectamine™ 2000 (Invitrogen, USA) for 72 h.

### FBXO7-interacting protein sequence analysis by immunoprecipitation mass spectrometry (IP-MS)

Nucleus pulposus cell lysates were subjected to immunoprecipitation using an anti-FBXO7 antibody, and the immunoprecipitated proteins were resolved by SDS-PAGE, excised as a single gel lane, and digested in-gel with trypsin. The resulting peptides were desalted on C18 StageTips and analyzed on a Q-Exactive HF mass spectrometer coupled to an UltiMate 3000 RSLCnano system, using a 60-min gradient and data-dependent acquisition (top 20). Raw MS data were processed with MaxQuant (version 2.2.0.0) and searched against the UniProt human reference proteome (downloaded 20250113) with trypsin/P specificity (up to two missed cleavages), carbamidomethyl (C) as a fixed modification, and oxidation (M), acetyl (protein N-term), and deamidation (NQ) as variable modifications. Mass tolerances were 20 ppm for first search and 4.5 ppm for main search (MS1), and 20 ppm for MS/MS. Peptide-spectrum match, protein, and site false discovery rates were all set to ≤1%.

### MED12-interacting protein sequence analysis by IP-MS

Nucleus pulposus cell lysates were subjected to immunoprecipitation using an anti-MED12 antibody, and the immunoprecipitated proteins were resolved by SDS-PAGE, excised as a single gel lane, and digested in-gel with trypsin. The resulting peptides were desalted on C18 StageTips and analyzed on a Q-Exactive Plus mass spectrometer coupled to an Easy-nLC 1200 system, using a 60-min gradient and data-dependent acquisition (top 20). Raw MS data were processed with MaxQuant (version 2.4.14.0) and searched against the UniProt human reference proteome (downloaded 2024-08-02) with trypsin specificity (up to two missed cleavages),

carbamidomethyl (C) as a fixed modification, and oxidation (M) and acetyl (protein N-term) as variable modifications. Mass tolerances were 20 ppm for first search and 4.5 ppm for main search (MS1), and 20 ppm for MS/MS. Peptide-spectrum match, protein, and site false discovery rates were all set to ≤1%.

**Western blotting**

After the indicated treatments, protein lysates were extracted using RIPA buffer (Boster, China) supplemented with PMSF (MedChemExpress, USA). Protein concentrations were quantified via a BCA assay (Boster, China), and equal amounts of protein (20–50 μg) were resolved by 8–12% SDS–PAGE under reducing conditions. The separated proteins were transferred to PVDF membranes (Millipore), which were blocked with 5% nonfat milk in TBST (Tris-buffered saline with 0.1% Tween-20) for 1 hour at room temperature, followed by incubation with primary antibodies overnight at 4 °C. After washing, the membranes were incubated with HRP-conjugated secondary antibodies for 1 hour at room temperature. The protein bands were visualized using enhanced chemiluminescence (ECL) substrate (Thermo Scientific) and imaged with a ChemiDoc system (Bio-Rad). Densitometric analysis was performed using ImageJ software (NIH), with GAPDH used as a loading control. All experiments included three biological replicates and were repeated at least twice independently.

**Reverse transcription quantitative polymerase chain reaction (RT–qPCR)**

Total RNA was isolated from cells or tissues using TRIzol reagent (Invitrogen) and quantified via NanoDrop spectrophotometry (Thermo Scientific). Reverse transcription was performed with 1 μg of RNA using the HiScript III RT SuperMix for qPCR (Vazyme, China) according to the manufacturer's protocol. qPCR was carried out in triplicate using SYBR Green Master Mix (Vazyme, China) on a CFX96 Touch sequence detection system (Bio-Rad, USA). Relative mRNA levels were calculated using the $2^{-\Delta\Delta Ct}$ method and normalized to the level of GAPDH. Further information on the primer sequences is provided in Supplementary Table 7.

**Chromatin Immunoprecipitation assays (ChIP).**

Cells were conducted with corresponding disposal. ChIP was conducted using a Simple ChIP Enzymatic Chromatin IP kit (Cell Signaling Technology), according to the manufacturer's instructions. Antibody of anti-HIF1A was used for immunoprecipitation. Normal rabbit IgG was used as a negative control. Primers of PRMT2 for ChIP-qPCR are listed in Supplementary Table 6.

**Generation of Anti- FBXO7-R504me Antibody**

The anti-FBXO7-R504me antibody (customized from HUABIO) was generated in rabbits using the peptide GGPNDR(me)FPFRP and ASPNNR(me)FPFRP as antigens. A total of five immunizations were performed. The first immunization dose was 0.75 mg, whereas half of the first dose was used for the next four immunizations. Finally, the serum was obtained for purification.

**Bulk-RNA sequencing and Gene set enrichment analysis (GSEA)**

Human nucleus pulposus (NP) cells were transfected with si-Scramble or si-MED12-1 (three biological replicates per group) for 48 h. Total RNA was extracted using TRIzol reagent (Thermo Fisher, USA). RNA integrity was assessed using an Agilent 2100 Bioanalyzer, and 1 μg

of total RNA per sample was used for library construction. Libraries were prepared using the MGIEasy RNA Library Prep Kit (MGI Tech, China) and sequenced on an MGISEQ-T7 platform (MGI Tech) with paired-end 150 bp reads, generating approximately 6 G of raw data per sample. Raw reads were quality-controlled using fastp (version 0.23.0). Clean reads were aligned to the human reference genome GRCh38.87. Gene-level read counts were quantified using featureCounts. Differential expression analysis was performed using DESeq2, with genes considered significantly differentially expressed if $|\log_2(\text{fold change})| > 1$ and adjusted p-value < 0.05.
GSEA was conducted using GSEA 4.3.2 software with 1000 permutations and default parameters according to standard procedure. The C2 (curated gene sets) collection and C5 (ontology gene set) collection of the Molecular Signatures Database (MSigDB) version 7.5.1 were used to map overlaps between gene sets in MSigDB and expression set.

**Co-immunoprecipitation (Co-IP)**
After indicated treatment, treated cells were lysed with NP-40 (Boster, China) supplemented with 1% Cocktail and 1% PMSF (MedChemExpres, USA) for 30 min on the ice, centrifuged at 12000 rpm for 15 min, and the protein content of supernatant was measured by BCA protein assay kit (Boster, China). 1000 μg proteins with the concentration of 1 μg/μl were used to incubate with protein A/G beads (MedChemExpres, USA) conjugated with specific primary antibodies at 4 ºC overnight on a rotator. And the immunoprecipitation was eluted by 1×loading buffer (Boster, USA) and analyzed by western blotting analysis as previous described.

**EdU Incorperation Assay**
EdU labeling was performed to examine the proliferation status of NPCs. NPCs were exposed to 25μM of 5-ethynyl-2′-deoxyuridine (EdU, RiboBio, C10338, Guangzhou, China) for 12h at 37°C and fixed in 4% paraformaldehyde. NPCs were then permeabilized using 0.5% Triton-X-100 and then reacted with Apollo488 for 30 mins. subsequently, Hoechst 33342 was used to stain the DNA contents of the cells for 30 min, and images were visualized and captured using a microscope (Olympus, BX53). EdU positive cells were analyzed using Image J. The experiments were replicated three times.

**R-loop detection using Dot-Blot**
Genomic DNA was extracted from NP cells using the TIANamp Genomic DNA Kit (TIANGEN, China) following the manufacturer's protocol. The concentration of DNA was determined using a spectrophotometer. The extracted DNA was then diluted to a standard con centration of 200ng/μl and subjected to further serial dilutions for detailed analysis. As a control, an aliquot of the DNA was also diluted to 200ng/μl in a reaction mixture containing 5units of RNase H (M0297, New England Biolabs) and are action buffer with a water base, to a final volume of 20μl, and then incubated in 37° for 20min. This control setup was similarly serially diluted. Subsequently, 2μl samples from each of these diluted DNA concentrations were carefully spotted onto a nitrocellulose membrane for further experimental processes. The membrane was air-dried for 1h at room temperature and cross-linked using a UV cross-linker (1200μJx100). To block nonspecific binding, the membrane was incubated with 5%nonfatdry milk in Tris-buffered saline with 0.1% Tween 20 (TBST) for 1h at room temperature. Next, the membrane was incubated overnight at 4°C with gentle shaking with an antibody specific to R-loops, S9.6 (Sigma, MABE1095, 1:200) antibody. After washing the membrane three times, it was incubated with a

secondary antibody. R-loop signals were visualized using an enhanced chemiluminescence (ECL) substrate.

**SA-β-galactosidase Staining**

SA-β-galactosidase staining was performed using a Senescence β-Galactosidase Staining Kit (Beyotime Biotechnology, C0602, Shanghai, China) according to the manufacturer's protocol. Briefly, NPCs were washed with PBS and fixed with the fixative provided in the kit for 20 min at room temperature. After removing the fixative and washing again with PBS, cells were incubated with freshly prepared staining solution at 37 ℃ for 12 h. Images were captured under a microscope (Olympus, BX53; Melville, NY, USA).

**Immunofluorescence**

NP cells were planted in the glass coverslip. After the medium was replaced twice, NP cells were exposed to indicated treatment. The cellular coverslip was washed twice with PBS, fixed with 4% paraformaldehyde for 20 min, permeabilized with 0.5% Triton-X-100 for 15 min, blocked with normal goat serum for 30 min, incubated with primary antibodies at 4 ℃ overnight, washed twice with PBS supplemented with 0.1% tween-20 and incubated with secondary antibodies of anti-mouse/rabbit Alexa Fluor 488 nm or 568 nm. Cellular nucleus was stained with DAPI (Invitrogen, USA). The fluorescent images were captured using confocal imaging (Olympus, FV3000).

**Identification of methylated protein and residues by mass spectrometry**

Arginine mono-methylated peptides were enriched by immunoprecipitation (IP) using asymmetric mono-methyl arginine (me-R) antibodies with protein A/G beads (MedChemExpres, USA) at 4 ℃ overnight on a rotator. After washed 5 times with pre-cooled NP-40 lysis buffer, immunoprecipitates were eluted with 1×loading buffer (Boster, USA) and separated SDS-PAGE gel. According to the manufacture's protocol, SDS-PAGE gel piece was decolorized, alkylated and enzymatically disintegrated. The samples were analyzed by liquid chromatography–tandem mass spectrometry (LC-MS/MS) on a Q Exactive mass spectrometer (Thermo Fisher Scientific). The LC-MS/MS data were processed using Proteome Discoverer (Thermo Fisher Scientific) and searched against the Swiss-prot Homo sapiens protein sequence database.

**EVs isolation and plasmid loading**

Rat bone marrow mesenchymal stem cells (rBMSCs) were obtained from the bilateral femurs of four-month-old SD rats, isolated by density gradient centrifugation and adhered to tissue culture plastic. rBMSCs were cultured in the 1:1 DMEM: F12 growth medium combined with 10% FBS and 1:100 penicillin-streptomycin in the incubator with 5% CO2 at 37 °C condition. The medium was changed every three days. After rBMSCs were passaged to second generation, the medium was replaced with 1:1 DMEM: F12 treated with 15% EV-free FBS (System Bioscience, USA) and collected for isolate EVs. EVs were purified according to the differential ultracentrifugation protocols (49, 88, 104, 105). Briefly, collected medium was centrifuged sequentially at 600×g for 10 min, 2000×g for 30 min and 10000×g for 30 min to remove dead cells or cell debris, and ultra-centrifuged at 20000×g for 60 min and washed twice with PBS to isolate EVs. Finally, EVs were suspended with PBS and stored in 4°C for further experiments. BCA protein assay kit (Boster, China) was using to measure the protein concentration of EVs. A total of 4 μg vector or

MED12-overexpressing plasmids were mixed with 200 μl EVs (100 μg/ml). Then the mixtures were transferred into 4 mm electroporation cuvettes and electroporated at 0.150 Kv/100 μF.

**EVs identification**

For observing the morphology of engineered EVs, a total of 20 μl EVs was loaded onto a formvar/carbon-coated grid for 5 min. after dried on bibulous paper, the grid was immediately negatively stained with 3% aqueous phosphotungstic acid for 1 min, and dried overnight. The grid was pictured using transmission electron microscopy (FEI Tecnai G20 TWIN, USA). For analyzing the concentration and size of engineered EVs, a total of 20 μl EVs were diluted 100- to 500-fold with precooled PBS for measurement. ZetaView Multiple Parameter Particle Tracking Analyzer (Particle Metrix) was using to assess the number and size of EVs via nanoparticle tracking analysis. For identifying protein markers of EVs, western blotting was used to analyze the protein content of EVs involved in EV-markers including CD9, CD63 and TSG101. Briefly, as described previously, protein concentration was measured by BCA protein assay kit and a total of 10 μg protein were separated on 10% SDS-PAGE gel, transferred to 0.45 μm PVDF membranes and incubate with special primary antibodies. Cellular proteins were used as positively condition. For evaluating the loading of MED12-overexpressing plasmids, a total of 200 μl EVs (100 μg/ml) was used to exact DNA cargo in engineered EVs via TIANamp Genomic DNA Kit (TIANGEN, China). Isolated DNA cargo was amplified by using the special primers of MED12 gene, and quantitatively analyzed by performing qPCR as previously described.

**Intradiscal injection of EVs**

After the initial coccygeal IVDs needle puncture, rats randomly and double-blindly assigned to 3 treatment groups with 5 rats in each group. After anesthesia with 3% pentobarbital, a total of 2 μl solution containing PBS, vector-EVs (100 μg/L) and MED12-EVs (100 μg/L) was slowly injected into the center of NP regions of Co6-7, Co7-8 and Co8-9 coccygeal IVDs by using a 33-gauge needle. Immediately, the rats were sacrificed for in vivo imaging analysis to confirm that engineered EVs were injected into the NP regions of coccygeal IVDs in vivo, and after one month, the rats were sacrificed for radiographic and histological analysis.

**Intradiscal injection of AAVs**

Three-month-old female Sprague-Dawley rats were randomly divided into multiple groups (n = 5 per group). After anaesthesia with 3% pentobarbital, a total of 2 μL of solution containing the indicated AAVs at a titer of $10^9$ plaque-forming units was slowly injected into the centre of the nucleus pulposus region of the Co6-Co7 and Co7-Co8 coccygeal intervertebral discs using a 33-gauge needle (Hamilton) attached to a microliter syringe (Hamilton). An adeno-associated virus (AAV) containing short hairpin RNA targeting PRMT2, MED12, HIF1A, FBXO7, or a scrambled sequence, as well as AAVs for overexpression of FBXO7 (wild-type or R504F mutant) or PRMT2, were generated. For ubiquitous expression, AAVs were constructed using the pAAV5-CMV-EGFP system according to the manufacturer's protocols. For nucleus pulposus (NP)-specific expression, AAVs were constructed using the AAV5-col2a1-T2A-mCherry system, in which the col2a1 promoter drives transgene expression specifically in NP cells. The AAV constructs driven by the CMV promoter included AAV-sh-Scramble, AAV-sh-HIF1A, AAV-sh-PRMT2-1, AAV-sh-PRMT2-2, AAV-sh-MED12-1, AAV-sh-MED12-2, and AAV-PRMT2. The AAV constructs driven by the col2a1 promoter

(NP-specific) included AAV-sh-FBXO7, AAV-FBXO7-WT, and AAV-FBXO7-RF. After one month, the rats were sacrificed for radiographic and histological analysis.

**Immunohistochemistry (IHC)**

Slides of human NP samples or rat coccygeal IVD specimens were deparaffinized with xylene, rehydrated with ethanol in gradient concentrations, antigen-retrieved with citrate buffer, blocked with normal goat serum, incubated with special primary antibodies overnight. After incubated with secondary antibodies and visualized with DAB peroxidase substrate kit, histological images were analyzed using the BX53 microscope (Olympus).

**Histological and Radiographic Evaluation and Analysis**

One months later, rats were sacrificed and histological and radiographic evaluation were performed. After X-ray and MRI examination, tails were fixed in 10% neutral-buffered formalin for 1 week and Midsagittal sections were stained with hematoxylin and Safranin O-fast green to evaluate the degeneration level. The histological evaluation was performed according to histologic grading system developed by Ji et al. More specifically, the cellularity and morphology of the AF, NP, and the border between the two structures were examined. The scale is based on 5 categories of degenerative changes with scores ranging from 0 points (0 in each category) for a normal disc to 15 points (3 in each category) for a severely degenerated disc. For morphology of the NP, score 0: round shape and the NP constitutes >75% of the disc area, score 1: round shape and the NP constitutes 50–75% of the disc area, score 2: round shape and the NP constitutes 25–50% of the disc area, score 3: round shape and the NP constitutes <25% of the disc area. For cellularity of the NP, score 0: stellar-shaped cells with a proteoglycan matrix located at the periphery, evenly distributed, score 1: partially stellar and partially round cells, more stellar than round, score 2: mostly large, round cells, separated by dense areas of proteoglycan matrix, score 3: large, round cells, separated by dense areas of proteoglycan matrix. For morphology of the AF, score 0: well-organized collagen lamellae with no ruptures, score 1: inward bulging, ruptured, or serpentine fibers constitute <25% of the AF, score 2: inward bulging, ruptured, or serpentine fibers constitute 25−50% of the AF, score 3: inward bulging, ruptured, or serpentine fibers constitute >50% of the AF. For cellularity of the AF, score 0: fibroblasts comprise >90% of the cells, score 1: fibroblasts comprise >75–90% of the cells, score 2: intermediate, score 3: chondrocytes comprise >75% of the cells. For border between the NP and AF, score 0: normal, without any interruption, score 1: minimal interruption, score 2: moderate interruption, score 3: severe interruption. Radiographs were taken at 4 weeks after the puncture. The change in IVD height was evaluated by the disc height index (DHI) The change in IVD height was evaluated by the disc height index (DHI) Measurements of internal control discs were carried out together with their corresponding punctured discs. Disc height and the adjacent vertebral body heights were measured on the midline and 25% of the disc's width from the midline on either side. The DHI was expressed as the mean of the 3 measurements from midline to the boundary of the central 50% of disc width divided by the mean of the 2 adjacent vertebral body heights. Changes in the DHI of punctured discs were expressed as a percentage (%DHI=post-punctured DHI/pre-punctured DHI ×100). MRI-based Pfirrmann grading system was applied to assess the degenerative grade of the NP specimens.

**Supplemental figure 1.**

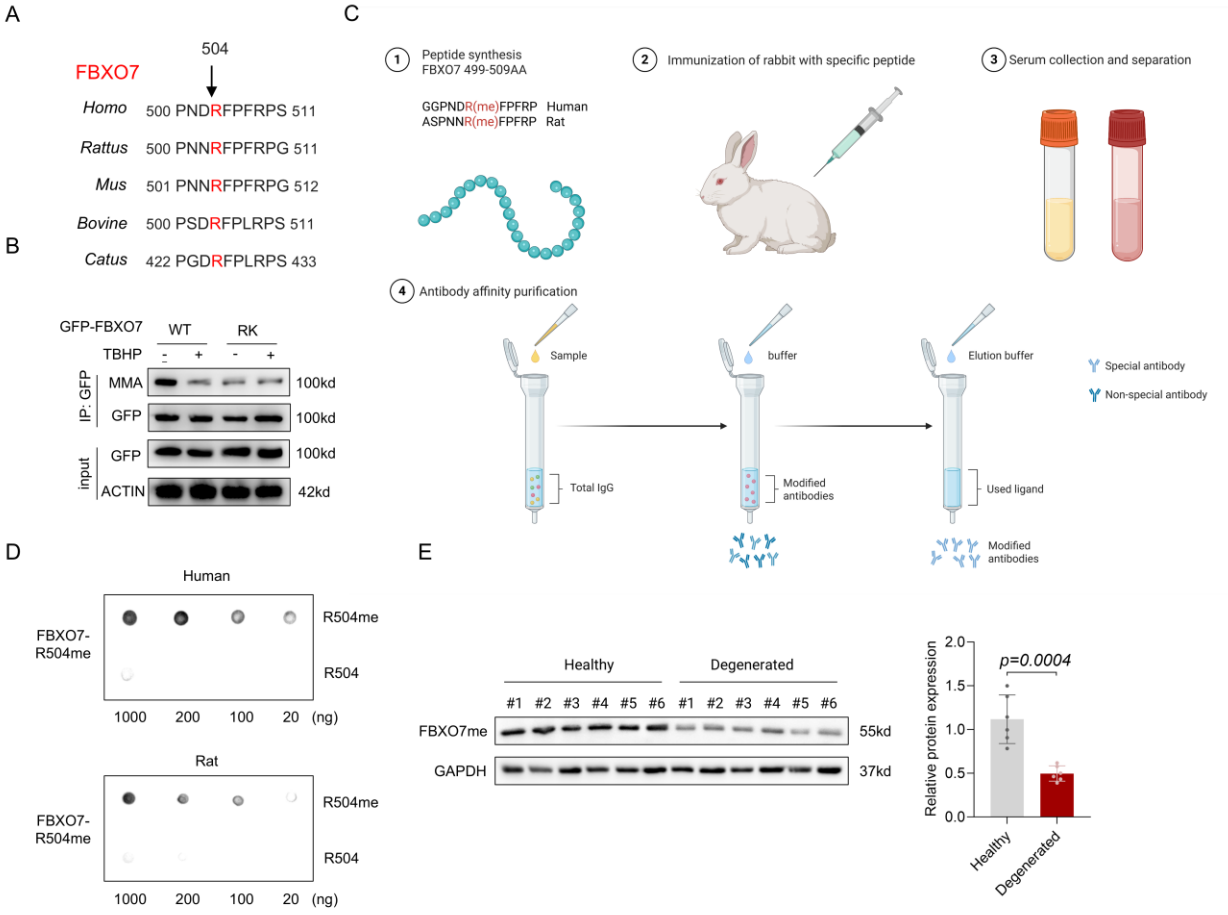


**Supplemental figure 1. (A)** Alignment of amino acid sequences of FBXO7 across all species showing Arg504 highlighted in red. **(B)** Co-IP analysis of methylated FBXO7 in NPCs transfected with GFP-tagged wild-type FBXO7 or FBXO7 RK mutants. **(C)** Schematic diagram of the experimental design for the generation of anti-FBXO7-R504me antibodies. **(D)** The specificity of the anti-FBXO7-R504me antibody was verified by dot blot. **(E)** Protein level analysis of FBXO7-R504me in human NP tissues by western blot. Unpair students' t test (**E**) was used to performed, and data are represented as mean ± SD. At least 3 independent experiments were performed.

## Supplemental figure 2.

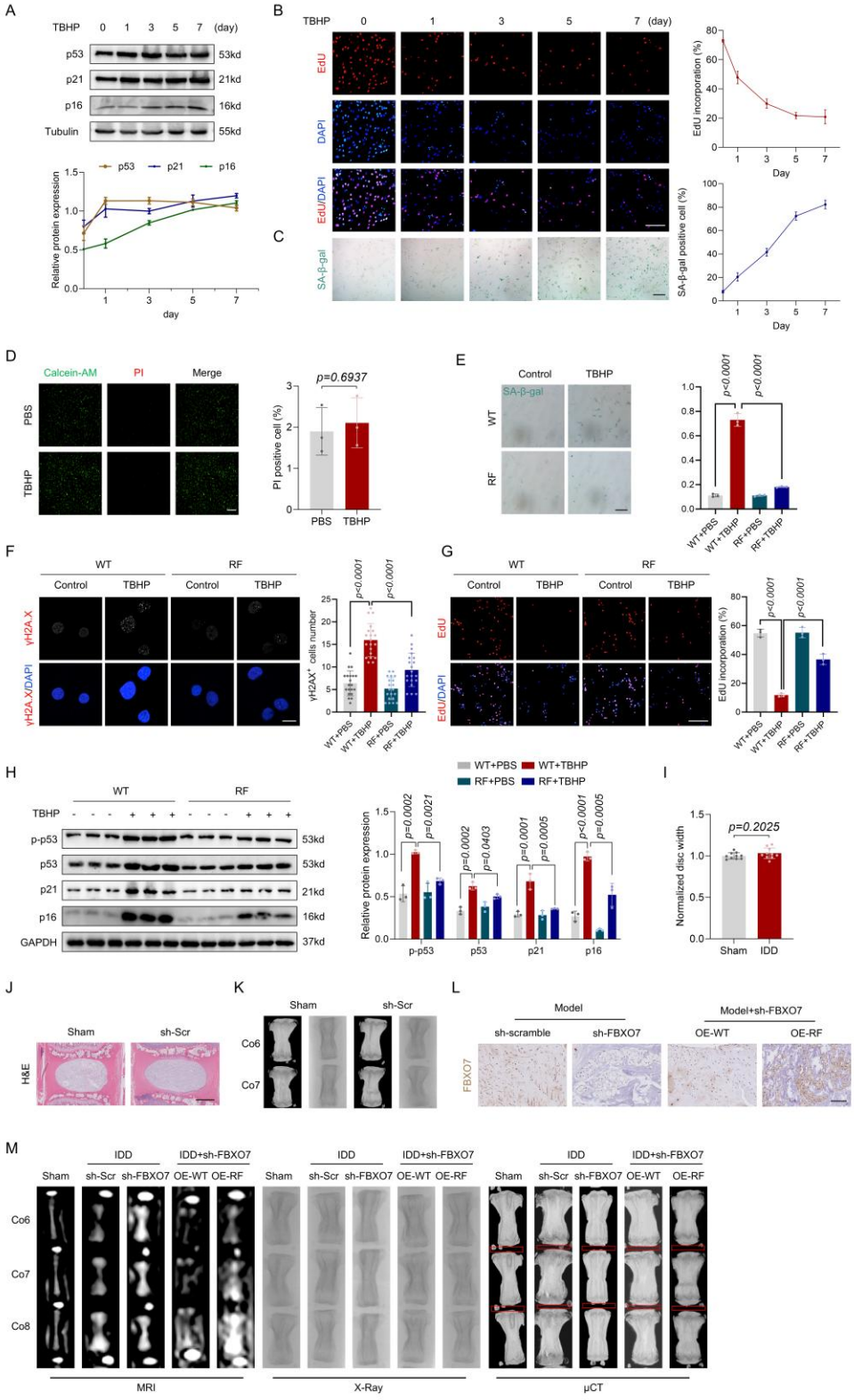

**Supplemental figure 2. (A)** Western blot analysis of p53, p21, p16 in human NPCs with the indicated treatment. **(B)** EdU incorporation assay and analysis of NPCs with the indicated treatment (Scale bar: 100 μm). **(C)** SA-β-gal activity staining and analysis of NPCs with the indicated treatment (Scale bar: 100 μm). **(D)** NPC viability was evaluated through live/dead fluorescence staining with the indicated treatment (Scale bar: 200 μm). (**E**) SA-β-gal activity staining and analysis of NPCs reconstituted expression of wild-type FBXO7 or FBXO7 RK mutant with the indicated treatment (Scale bar: 100 μm). (**F**) IF staining of γH2A.X foci and analysis of NPCs reconstituted expression of wild-type FBXO7 or FBXO7 RK mutant with the indicated treatment (Scale bar: 10 μm). (**G**) EdU incorporation assay and analysis of NPCs reconstituted expression of wild-type FBXO7 or FBXO7 RK mutant with the indicated treatment (Scale bar: 100 μm). (**H**) Western blot analysis of p-p53, p53, p21, p16 in human NPCs reconstituted expression of wild-type FBXO7 or FBXO7 RK mutant with the indicated treatment. (**I**) Disc width was measured on H&E-stained mid-sagittal sections and normalized to disc width measured on X-ray images. (**J**) H&E staining of coccygeal vertebrae from rats with the indicated treatment (Scale bar: 1 mm). (**K**) Representative X-ray images, μCT images of coccygeal vertebrae and IVDs from rats with the indicated treatment. (**L**) IHC staining analysis of the knockdown efficiency of sh-FBXO7 in NP tissues, and the overexpression efficiency of WT and RF mutant FBXO7 in NP tissues. (**M**)Representative X-ray images, μCT images, MRI images of coccygeal vertebrae and IVDs from rats with the indicated treatment. Unpair students' t test (**D**, **I**) was used to performed. One-way ANOVA (**E**, **F**, **G**, **H**) was used to performed, and data are represented as mean ± SD. At least 3 independent experiments were performed.

## Supplemental figure 3.

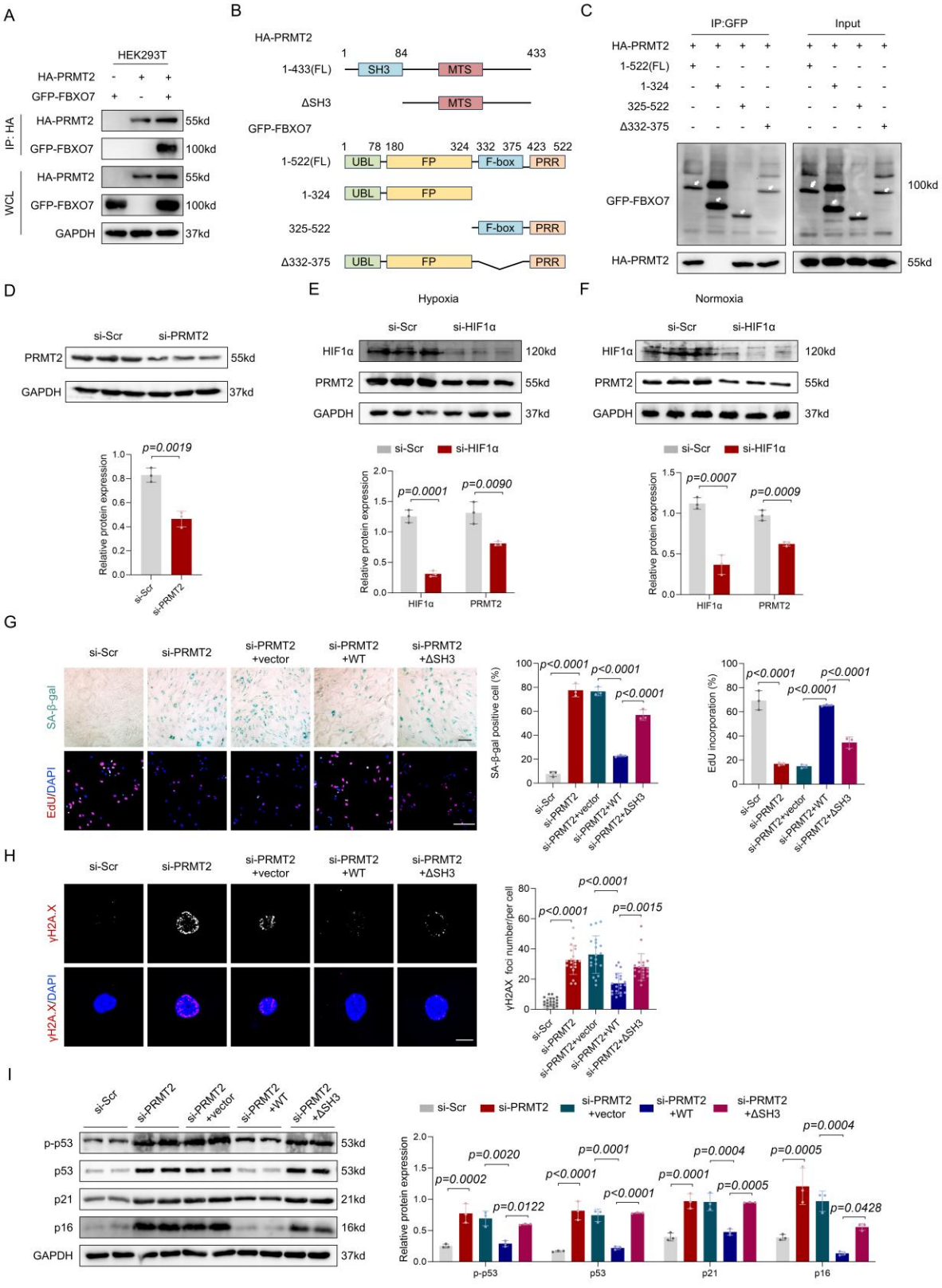

**Supplemental figure 3.** (**A**) Exogenous Co-IP analysis of the interaction of FBXO7 with PRMT2 in HEK293T cells cotransfected with GFP-FBXO7 and HA-PRMT2. (**B**) A schematic presentation of FBXO7 and PRMT2 domains. (**C**) GFP-FBXO7 FL or indicated truncation mutants were co-expressed with HA-PRMT2 in HEK293T cells. Proteins were immunoprecipitated using GFP antibody and analyzed by western blotting. (**D**) Western blot analysis of PRMT2 in NPCs with PRMT2 silencing. (**E**) Western blot analysis of PRMT2 and HIF1α in NPCs with HIF1α silencing under hypoxia. (**F**) Western blot analysis of PRMT2 and HIF1α in NPCs with HIF1α silencing under normoxia. (**G**) SA-β-gal activity staining and EdU incorporation assay of NPCs with PRMT2 silencing accompanied with overexpression of wild-type or mutant PRMT2 (Scale bar: 100 μm). **(H)** IF staining of γH2A.X foci and analysis of NPCs with PRMT2 silencing accompanied with overexpression of wild-type or mutant PRMT2 (Scale bar: 10 μm). (**I**) Western blot analysis of p-p53, p53, p21, p16 in human NPCs with PRMT2 silencing accompanied with overexpression of wild-type or mutant PRMT2 by western blot. Unpair students' t test (**D, E, F**) were used to performed, and data are represented as mean ± SD. One-way ANOVA (**G**, **H, I**) was used to performed, and data are represented as mean ± SD. At least 3 independent experiments were performed.

**Supplemental figure 4.**

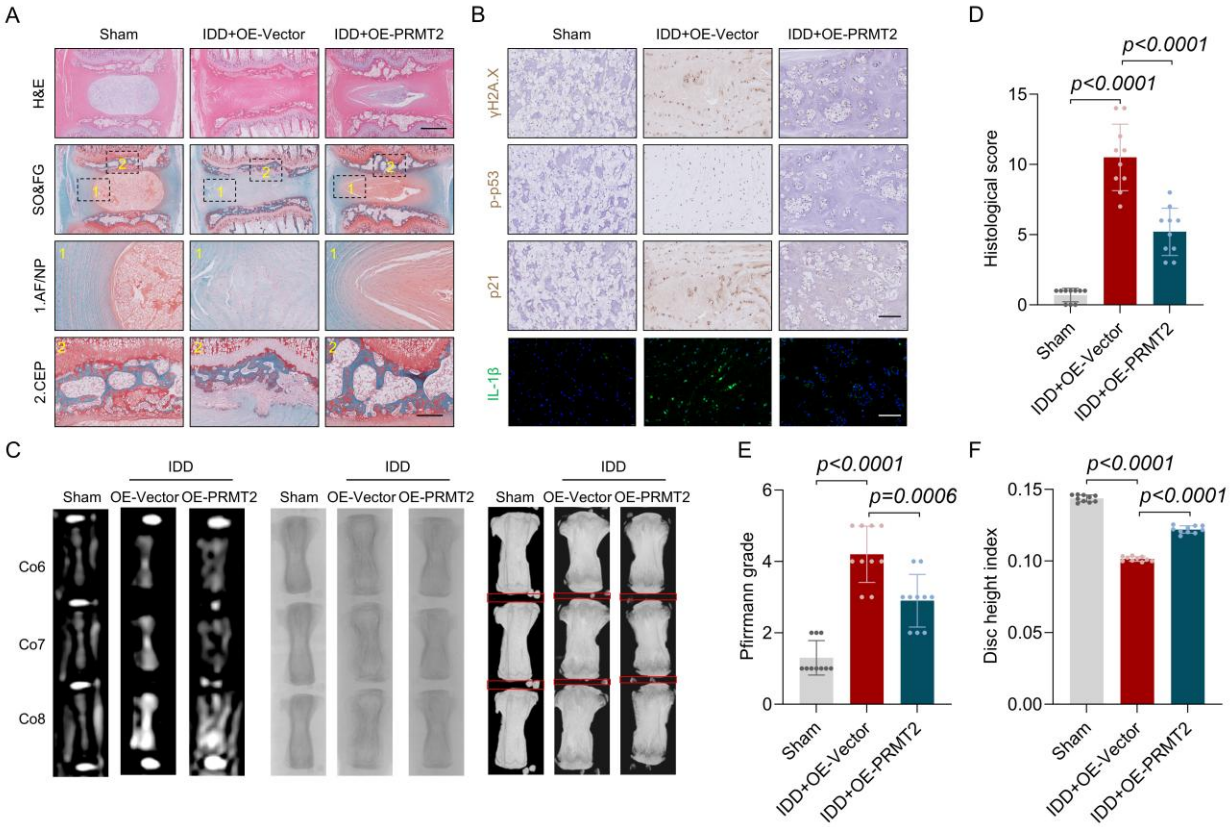


**Supplemental figure 4.** (**A**) H&E staining SO&FG staining of coccygeal vertebrae from rats with the indicated treatment (Scale bar: 1 mm, 250 μm). (**B**) IHC staining and IF staining of p-p53, γH2A.X, p21 and IL-1β in rat coccygeal IVDs (Scale bar: 100 μm) (**C**) Representative X-ray, μCT images and MRI images of coccygeal vertebrae from rats with the indicated treatment. Representative (**D**) Histological score (n = 10), (**E**) Pfirrmann degenerative grades (n = 10) and (**F**) disc height index (n = 10) of rat coccygeal IVDs. One-way ANOVA (**D**, **E**, **F**) was used to performed, and data are represented as mean ± SD. At least 3 independent experiments were performed.

**Supplemental figure 5.**

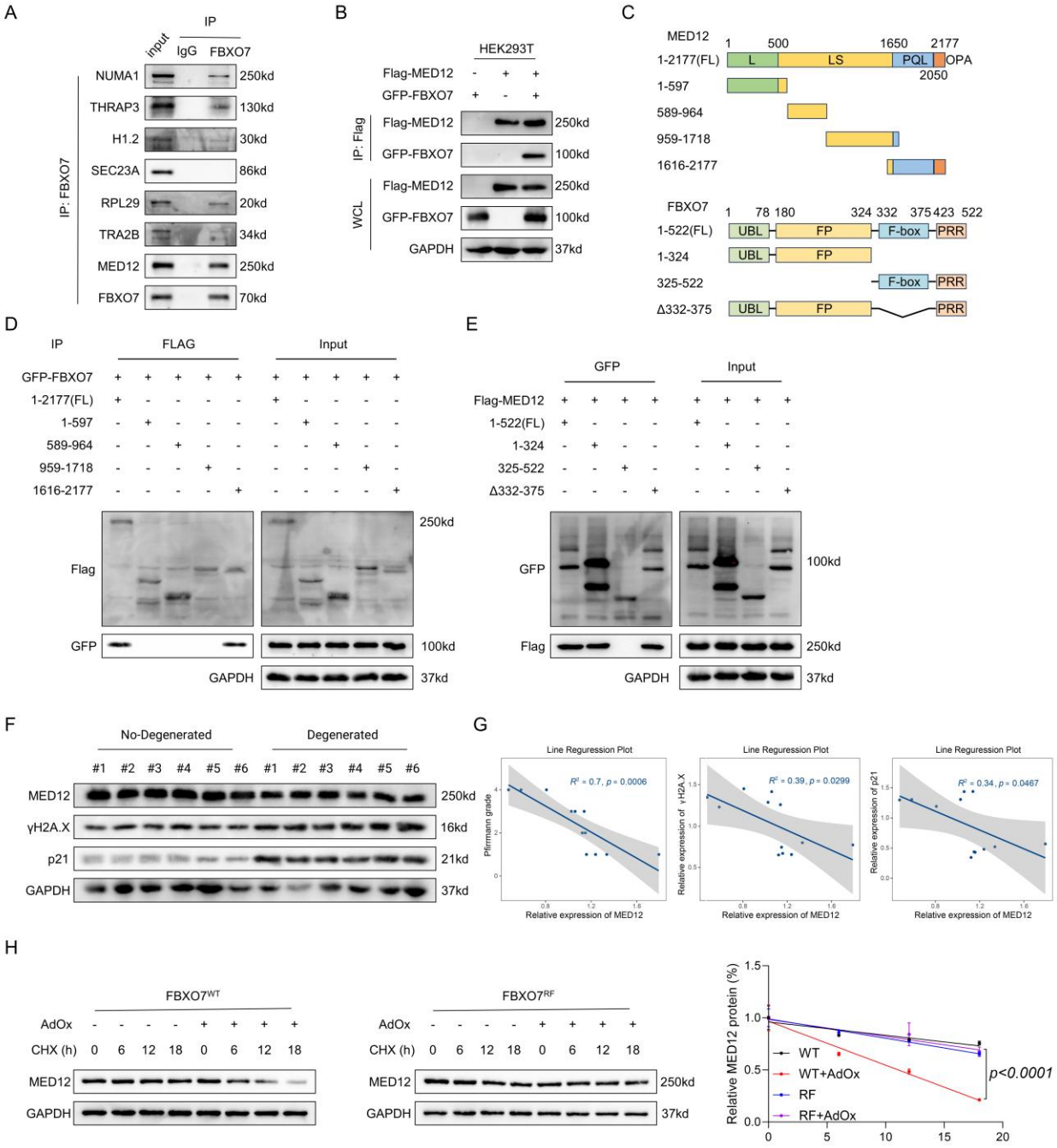


**Supplemental figure 5.** (**A**) Endogenous Co-IP analysis of the interaction of FBXO7 with 7 protein identified by IP-MS in NPCs. (**B**) Exogenous Co-IP analysis of the interaction of FBXO7 with MED12 in HEK293T cells cotransfected with GFP-FBXO7 and Flag-MED12. (**C**) A schematic presentation of FBXO7 and PRMT2 domains. (**D**) Flag-MED12 FL or indicated truncation mutants were co-expressed with GFP-FBXO7 in HEK293T cells. Proteins were

immunoprecipitated using Flag antibody and analyzed by western blotting. (**E**) GFP-FBXO7 FL or indicated truncation mutants were co-expressed with Flag-MED12 in HEK293T cells. Proteins were immunoprecipitated using GFP antibody and analyzed by western blotting. (**F**) Protein level analysis of MED12, γH2A.X, p21 in human NP tissues by western blot. (**G**) Linear regression analysis between the MED12 protein levels and the Pfirrmann MRI grades, linear regression analysis between the MED12 protein levels and the γH2A.X, p21 protein levels. (**H**) Half-life analysis of MED12 protein in HEK293T cells cotransfected with Flag-MED12 and GFP-FBXO7 (wild-type, RF mutants) with the indicated treatment. Simple linear regression (**G**) was used to performed. One-way ANOVA (**H**) was used to performed, and data are represented as mean ± SD. At least 3 independent experiments were performed.

**Supplemental figure 6.**

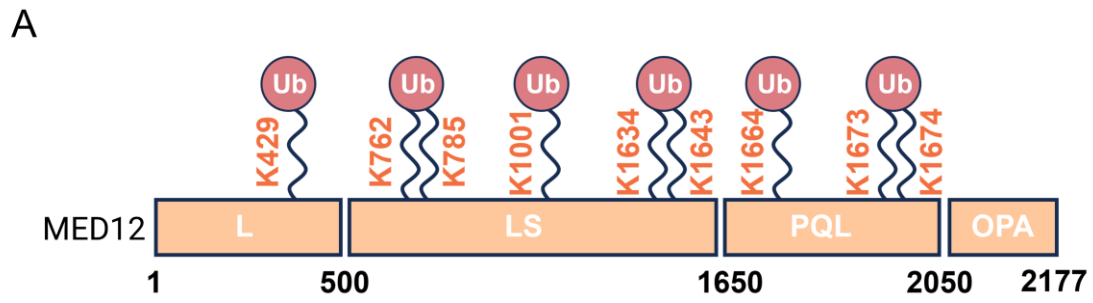


**Supplemental figure 6. (A)** Ubiquitination sites in MED12 protein predicted by GPS-Uber.

**Supplemental figure 7.**

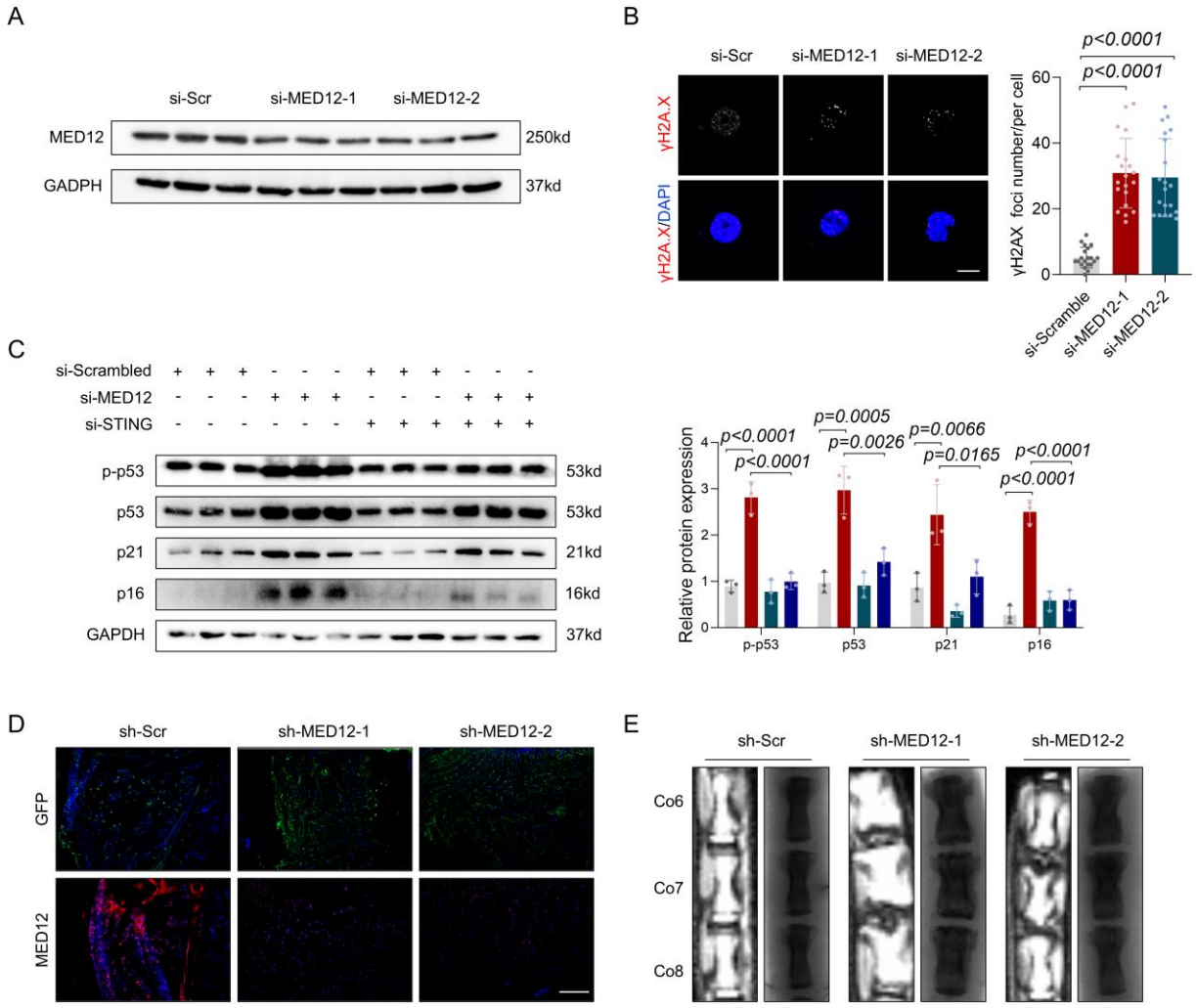


**Supplemental figure 7. (A)** Protein level analysis of MED12 in NPCs after treatment with specific siRNAs targeting MED12 by western blot. **(B)** γH2A.X foci analysis of NPCs with the indicated treatment (Scale bar: 10 μm). **(C)** Protein level analysis of p-p53, p53, p21, p16 in NP cells with the indicated treatment. **(D)** IF staining of GFP and MED12 of coccygeal vertebrae from rats with the indicated treatment (Scale bar: 100 μm). **(E)** Representative X-ray and MRI images of coccygeal vertebrae from rats with the indicated treatment. One-way ANOVA (**B**, **C**) was used to performed, and data are represented as mean ± SD. At least 3 independent experiments were performed.

**Supplemental figure 8.**

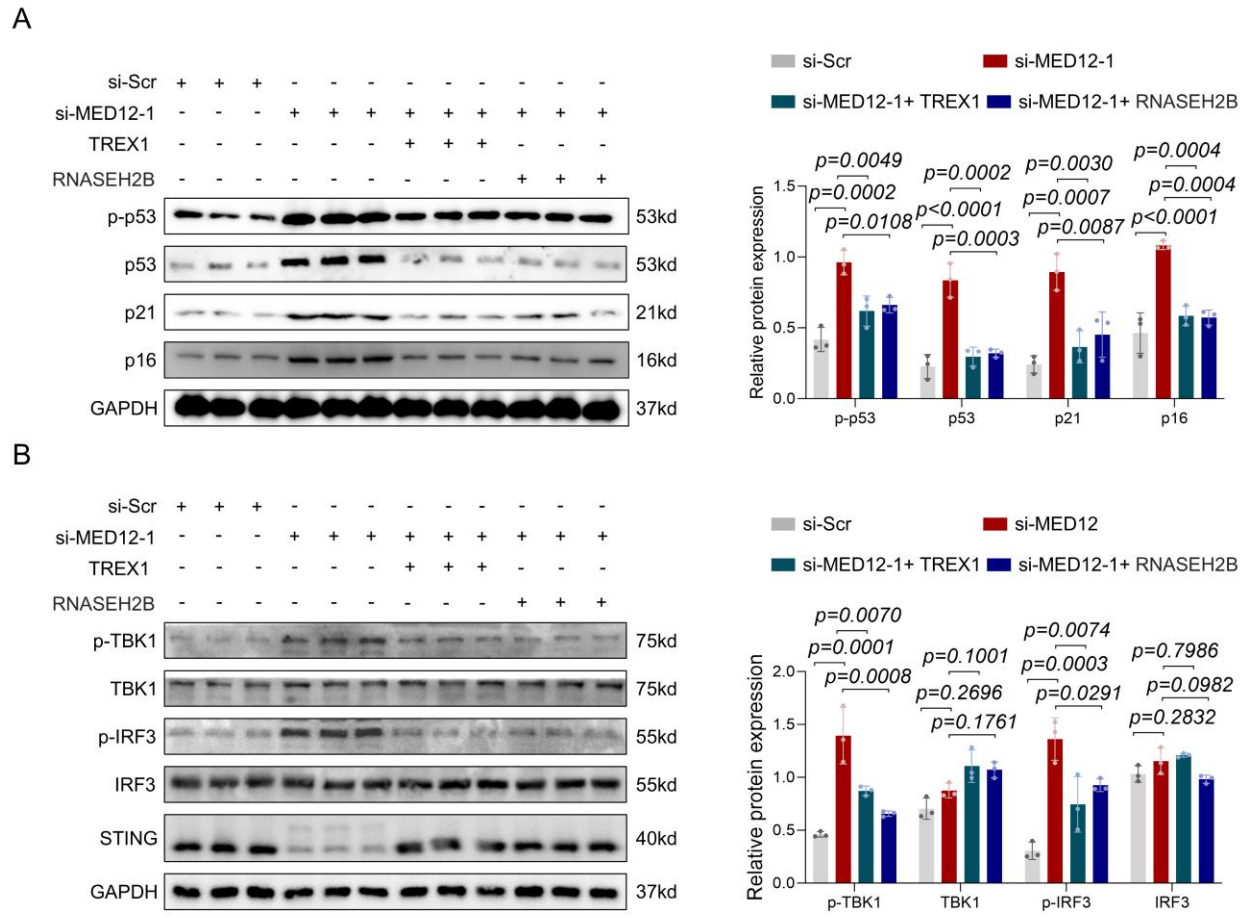


**Supplemental figure 8. (A)** Protein level analysis of p-p53, p53, p21, p16 in NP cells with the indicated treatment by western blot. **(B)** Protein level analysis of p-TBK1, TBK1, p-IRF3, IRF3, STING in NP cells with the indicated treatment by western blot. One-way ANOVA (**A**, **B**) was used to performed, and data are represented as mean ± SD. At least 3 independent experiments were performed.

**Supplemental figure 9.**

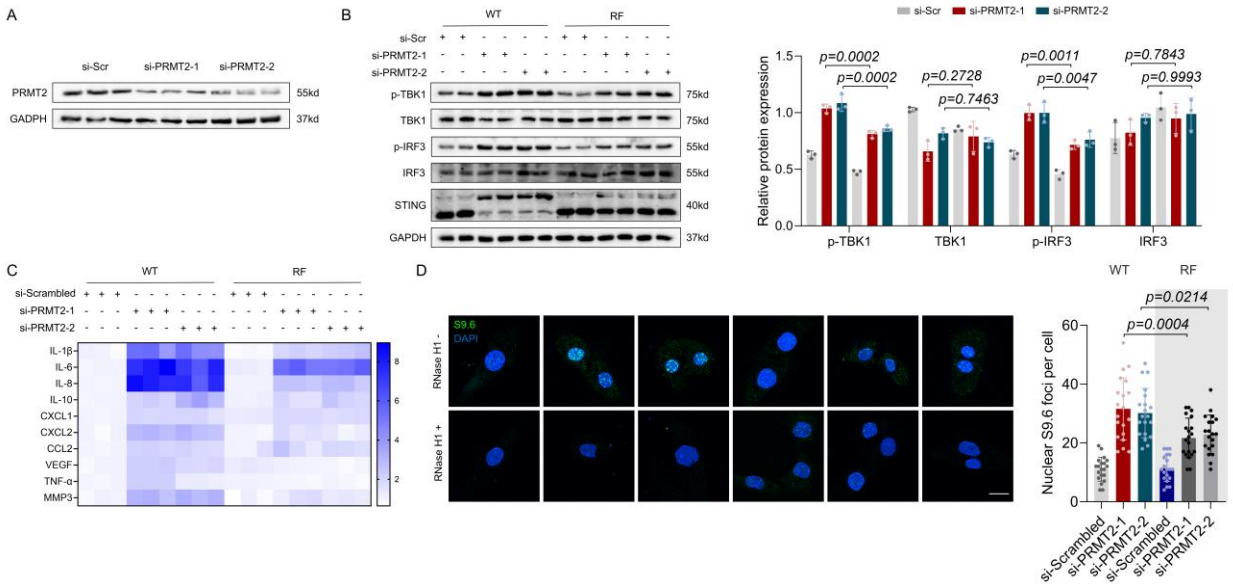


**Supplemental figure 9.** (**A**) Protein level analysis of PRMT2 in NPCs after treatment with specific siRNAs targeting PRMT2 by western blot. (**B**) Protein level analysis of p-TBK1, TBK1, p-IRF3, IRF3, STING in NP cells with the indicated treatment by western blot. (**C**) Heatmap of differential SASP in NP cells with the indicated treatment. (**D**) IF staining of R-loop in NP cells with the indicated treatment. RNaseH1 treatment was included as a negative control (Scale bar: 10 μm). One-way ANOVA (**B**, **D**) was used to performed, and data are represented as mean ± SD. At least 3 independent experiments were performed.

**Supplemental figure 10.**

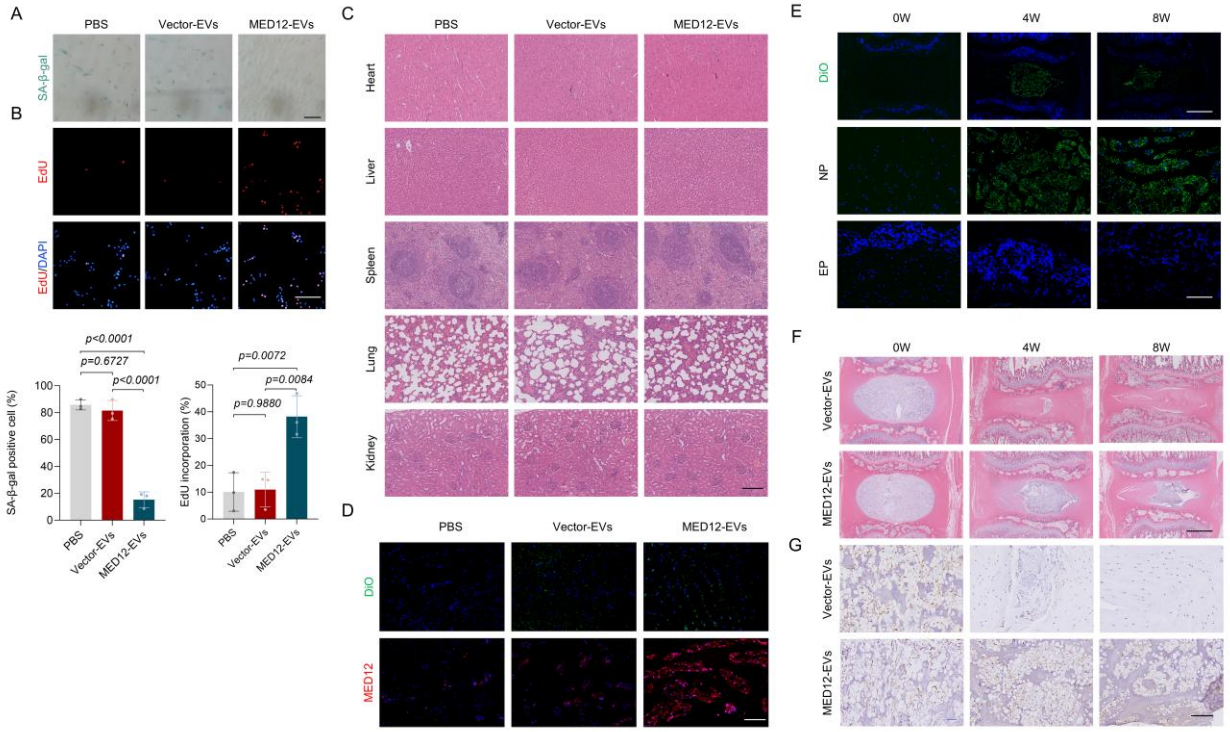


**Supplemental figure 10.** (**A and B**) SA-β-gal activity staining and EdU incorporation assay of rat NP cells with the indicated treatment (Scale bar: 100 μm). (**C**) H&E staining of lung, liver, spleen, kidney and heart of rats with the indicated treatment (Scale bar: 200 μm). (**D**) IF staining of DiO and MED12 of coccygeal vertebrae from rats with the indicated treatment (Scale bar: 100 μm) (**E**) IF staining of DiO of coccygeal vertebrae from rats with the indicated treatment (1 mm, 250 μm). (**F**) H&E staining of coccygeal vertebrae from rats with the indicated treatment (Scale bar: 1 mm). (**G**) IHC staining of MED12 in coccygeal vertebrae from rats with the indicated treatment (Scale bar: 100 μm). One-way ANOVA (**A**, **B**) was used to performed, and data are represented as mean ± SD. At least 3 independent experiments were performed.

**Supplementary Table 1. Characteristics details of the volunteers for label-free quantitative arginine methylated proteomics**

| Case Number | Gender | Age (years) | Pfirrmann grade | Diagnosis |
|---|---|---|---|---|
| Case 1 | Female | 12 | I | Idiopathic scolios |
| Case 2 | male | 17 | I | Idiopathic scolios |
| Case 3 | Female | 11 | I | Idiopathic scolios |
| Case 4 | male | 67 | IV | Lumbar disc herniation |
| Case 5 | Female | 64 | IV | Lumbar disc herniation |
| Case 6 | male | 74 | IV | Lumbar disc herniation |

**Supplementary Table 2. Characteristics details of the volunteers for FXBO7-R504me western blotting analysis**

| Case Number | Gender | Age (years) | Pfirrmann grade | Diagnosis |
|---|---|---|---|---|
| Case 1 | Female | 41 | II | Lumbar disc herniation |
| Case 2 | male | 24 | I | Lumbar vertebral fracture |
| Case 3 | Female | 31 | II | Lumbar disc herniation |
| Case 4 | Female | 18 | I | Idiopathic scoliosis |
| Case 5 | Female | 24 | II | Lumbar vertebral fracture |
| Case 6 | male | 46 | II | Lumbar disc herniation |
| Case 7 | male | 41 | IV | Lumbar spinal stenosis |
| Case 8 | male | 39 | IV | Lumbar spinal stenosis |
| Case 9 | Female | 32 | III | Lumbar disc herniation |
| Case 10 | Female | 21 | III | Lumbar disc herniation |
| Case 11 | male | 47 | IV | Lumbar disc herniation |
| Case 12 | male | 42 | V | Lumbar spondylolisthesis |

**Supplementary Table 3. Characteristics details of the volunteers for Co-IP analysis**

| Case Number | Gender | Age (years) | Pfirrmann grade | Diagnosis |
|---|---|---|---|---|
| Case 1 | Female | 11 | I | Idiopathic scolios |
| Case 2 | male | 14 | I | Idiopathic scolios |
| Case 3 | Female | 11 | I | Idiopathic scolios |
| Case 4 | Female | 18 | I | Idiopathic scolios |
| Case 5 | Female | 24 | I | Idiopathic scolios |
| Case 6 | male | 26 | II | Idiopathic scolios |
| Case 7 | male | 41 | III | Lumbar disc herniation |
| Case 8 | male | 49 | IV | Lumbar disc herniation |
| Case 9 | Female | 52 | III | Lumbar disc herniation |
| Case 10 | Female | 43 | III | Lumbar disc herniation |
| Case 11 | male | 47 | IV | Lumbar disc herniation |
| Case 12 | male | 62 | IV | Lumbar disc herniation |

**Supplementary Table 4. Characteristics details of the volunteers for western blotting analysis**

| Case Number | Gender | Age (years) | Pfirrmann grade | Diagnosis |
|---|---|---|---|---|
| Case 1 | male | 19 | I | Idiopathic scolios |
| Case 2 | Female | 17 | I | Idiopathic scolios |
| Case 3 | Female | 11 | I | Idiopathic scolios |
| Case 4 | Female | 14 | I | Idiopathic scolios |
| Case 5 | Female | 22 | I | Idiopathic scolios |
| Case 6 | Female | 21 | II | Idiopathic scolios |
| Case 7 | male | 51 | III | Lumbar disc herniation |
| Case 8 | Female | 39 | IV | Lumbar disc herniation |
| Case 9 | male | 62 | III | Lumbar disc herniation |
| Case 10 | Female | 78 | III | Lumbar disc herniation |
| Case 11 | male | 77 | IV | Lumbar disc herniation |
| Case 12 | male | 52 | IV | Lumbar disc herniation |

**Supplementary Table 5. Classification of Disc Degeneration**

| Grade | Structure | Distinction of Nucleus and Anulus | Signal Intensity | Height of Intervertebral Disc |
|---|---|---|---|---|
| I | Homogeneous, bright white | Clear | Hyperintense, isointense to cerebrospinal fluid | Normal |
| II | Inhomogeneous with or without horizontal bands | Clear | Hyperintense, isointense to cerebrospinal fluid | Normal |
| III | Inhomogeneous, gray | Unclear | Intermediate | Normal to slightly decreased |
| IV | Inhomogeneous, gray to black | Lost | Intermediate to hypointense | Normal to moderately decreased |
| V | Inhomogeneous, black | Lost | Hypointense | Collapsed disc space |

**Supplementary Table 6. Primer sequences used in Primers used for ChIP**

| Oligonucleotide | Sense (5'-3') | Antisense (3'-5') |
|---|---|---|
| Homo PRMT2 | ATTTTGTGGCTCGTAGGGGT | GTGGAGCTCGTCCCCAATC |

**Supplementary Table 7. Primer sequences used in PCR genotyping**

| Oligonucleotide | Sense (5'-3') | Antisense (3'-5') |
|---|---|---|
| Homo IL-1β | GGTTGAGTTTAAGCCAATCCA | TGCTGACCTAGGCTTGATGA |
| Homo IL-6 | GCCCAGCTATGAACTCCTTCT | GAAGGCAGCAGGCAACAC |
| Homo IL-8 | AGACAGCAGAGCACACAAGC | ATGGTTCCTTCCGGTGGT |
| Homo IL-10 | TGCCTTCAGCAGAGTGAAGA | GCTTGGCAACCCAGGTAA |
| Homo CXCL1 | GCTGAACAGTGACAAATCCAAC | CTTCAGGAACAGCCACCAGT |
| HomoCXCL2 | CCCATGGTTAAGAAAATCATCG | CTTCAGGAACAGCCACCAAT |
| Homo CCL2 | AGTCTCTGCCGCCCTTCT | GTGACTGGGGCATTGATTG |
| Homo TNF-α | CAGCCTCTTCTCCTTCCTGAT | GCCAGAGGGCTGATTAGAGA |
| Homo VEGF | AGGGCAGAATCATCACGAAGT | AGGGTCTCGATTGGATGGCA |
| Homo MMP3 | CAAAACATATTTCTTTGTAGAGGACAA | TTCAGCTATTTGCTTGGGAA |
| Homo GAPDH | CAAGAAGGTGAAGCAGG | TCAAAGGTGGAGGAGTGGGT |

**Supplementary Table 8. Oligonucleotide sequences used in this study**

| Sequence name | Forward (5′-3′) | Reverse (5′-3′) |
|---|---|---|
| Homo-si-Scrambled | UUCUCCGAACGUGUCACGUTT | ACGUGACACGUUCGGAGAATT |
| Homo-si-MED12-1 | CAGCAUUAUUGCAGAGAAATT | UUUCUCUGCAAUAAUGCUGTT |
| Homo-si-MED12-2 | CCGCAAAGGGACAGCAGAATT | UUCUGCUGUCCCUUUGCGGTT |
| Homo-si-Scrambled | GGAACUUGGCAACGUGUCUTT | AGACACGUUGCCAAGUUCCTT |
| Homo-si-PRMT2-1 | CAGUUGUGUUGCAGAGAAATT | UUUCUCUGCAACACAACUGTT |
| Homo-si-PRMT2-2 | GUGUCAUCCUGCAGAAUAATT | UUAUUCUGCAGGAUGACACTT |
| Homo-si-Scrambled | GCAAUAGGUGCAGAUAGAGTT | CUCUAUCUGCACCUAUUGCTT |
| Homo-si-FBXO7 | GAAUGACGACAGUAUGUUATT | UAACAUACUGUCGUCAUUCTT |
| Homo-si-Scrambled | UUCUCCGAACGUGUCACGUTT | ACGUGACACGUUCGGAGAATT |
| Homo-si-STING | GCAUUACAACAACCUGCUATT | UAGCAGGUUGUUGUAAUGCTT |

**Supplementary Table 9. Sequences of the shRNAs targeting rat mRNA transcripts**

| Target Gene | Clone name name | Sequence |
|---|---|---|
| Scrambled | Rat-sh-Scrambled | 5′-GACGGAATATGCGACTATGGT-3′ |
| PRMT2 | Rat-sh-PRMT2-1 | 5′-CGGTGGTGTTACAGAGAAATC-3′ |
| | Rat-sh-PRMT2-2 | 5′-TAGCAATCAAGGAGTTCTTTTCA-3′ |
| Scrambled | Rat-sh-Scrambled | 5′-GAGCACTAGCGCTGTTAATTA-3′ |
| MED12 | Rat-sh-MED12-1 | 5′-GCAAGATCTCAGAGTGCTATT-3′ |
| | Rat-sh-MED12-2 | 5′-CGACTGTTGCTCTACCATACC-3′ |
| Scrambled | Rat-sh-Scrambled | 5′-GAGCACTAGCGCTGTTAATTA-3′ |
| FBXO7 | Rat-sh-FBXO7 | 5′-CATTCCTCTCTCCAGAATAAT-3′ |
| Scrambled | Rat-sh-Scrambled | 5′-GTCTCCGAACGTGTCACGT-3′ |
| HIF1A | Rat-sh-HIF1A | 5′-GCAGACCCAGTTACAGAAACC-3′ |

**Supplementary Table 10. Antibody information**

| Antibody | Company | Catalog# | Application/ Dilution |
|---|---|---|---|
| anti-p16INK4a | Affinity | AF5484 | WB (1: 500) |
| anti-p21 | CST | 2947 | WB (1: 500) |
| anti-Phospho-p53 (Ser15) | Abcam | ab278683 | WB (1: 1000); IHC (1:150) |
| anti-p53 | CST | 9282 | WB (1: 1000) |
| anti-Phospho-γH2A.X (S139) | Abcam | ab81299 | IHC (1:150); WB (1:500); IF (1:250) |
| anti-STING | Proteintech | 19851-1-AP | WB (1:1000) |
| anti-ubiquitin | Abcam | ab134953 | WB (1: 500) |
| anti-mono-Methyl Arginine | CST | 8711 | WB (1:1000) |
| FBXO7 | CST | 57981 | WB (1: 1000); IP (4 μg/1000 μg) |
| PRMT2 | Proteintech | 66885-1-Ig | WB (1: 1000); IP (4 μg/1000 μg) |
| anti-GAPDH | Proteintech | 60004-1-Ig | WB (1: 2000) |
| anti-β-actin | Proteintech | 66009-1-Ig | WB (1: 2000) |
| anti-MED12 | Proteintech | 20028-1-AP | WB (1: 1000); IP (4 μg/1000 μg) |
| anti-S9.6 | Sigma-Aldrich | MABE1095 | Dot blot (1: 200); IF: (1: 100) |
| anti-ssDNA | Sigma-Aldrich | ZMS1042 | IF (1:100) |
| anti-CD63 | Proteintech | 25682-1-AP | WB (1: 500) |
| anti-CD9 | Proteintech | 20597-1-AP | WB (1: 2000) |
| anti-TSG101 | Proteintech | 28283-1-AP | WB (1: 1000) |
| anti-Flag tag epitope | Proteintech | 66008-4-Ig | WB (1: 20000); IP (4 μg/1000 μg) |
| anti-HA tag | Proteintech | 51064-2-AP | WB (1: 5000); IP (4 μg/1000 μg) |
| anti-GFP tag | Proteintech | 50430-2-AP | WB (1: 1000); IP (4 μg/1000 μg) |
| anti- NUMA1 | Proteintech | 16607-1-AP | WB (1: 500) |
| anti-THRAP3 | Proteintech | 19744-1-AP | WB (1: 500) |
| anti-Histone H1.2 | Proteintech | 19649-1-AP | WB (1: 500) |
| anti-TRA2B | Proteintech | 29627-1-AP | WB (1: 1000) |
| anti-SEC23A | Proteintech | 30465-1-AP | WB (1: 500) |
| anti-RPL29 | Proteintech | 15799-1-AP | WB (1: 2000) |
| anti-TBK1 | Proteintech | 67211-1-Ig | WB (1: 500) |
| anti-Phospho-TBK1(Ser172) | CST | 5483T | WB (1: 1000) |
| anti-FBXO7-R504me | HUABIO | N/A | WB (1: 1000) |
| anti-IRF3 | HUABIO | ET1612-14 | WB (1: 2000) |
| anti-Phospho-IRF3 (S396) | HUABIO | HA722772 | WB (1: 1000) |
| anti-HIF1a | Proteintech | 20960-1-AP | WB (1: 1000); IP (4 μg/1000 μg) |

**Supplementary Table 11. FBXO7 interactome in RK-mutant expressing cells.**

| Accession | GeneName | Description |
|---|---|---|

| | | |
|---|---|---|
| A0A075B6R9 | IGKV2D-24 | Probable non-functional immunoglobulin kappa variable 2D-24 OS=Homo sapiens OX=9606 GN=IGKV2D-24 PE=1 SV=1 |
| A0A087WW87 | IGKV2-40 | Immunoglobulin kappa variable 2-40 OS=Homo sapiens OX=9606 GN=IGKV2-40 PE=3 SV=2 |
| A7MCY6 | TBKBP1 | TANK-binding kinase 1-binding protein 1 OS=Homo sapiens OX=9606 GN=TBKBP1 PE=1 SV=1 |
| A8MTJ3 | GNAT3 | Guanine nucleotide-binding protein G(t) subunit alpha-3 OS=Homo sapiens OX=9606 GN=GNAT3 PE=2 SV=2 |
| O00423 | EML1 | Echinoderm microtubule-associated protein-like 1 OS=Homo sapiens OX=9606 GN=EML1 PE=1 SV=3 |
| O00567 | NOP56 | Nucleolar protein 56 OS=Homo sapiens OX=9606 GN=NOP56 PE=1 SV=4 |
| O14654 | IRS4 | Insulin receptor substrate 4 OS=Homo sapiens OX=9606 GN=IRS4 PE=1 SV=1 |
| O14732 | IMPA2 | Inositol monophosphatase 2 OS=Homo sapiens OX=9606 GN=IMPA2 PE=1 SV=1 |
| O14950 | MYL12B | Myosin regulatory light chain 12B OS=Homo sapiens OX=9606 GN=MYL12B PE=1 SV=2 |
| O15144 | ARPC2 | Actin-related protein 2/3 complex subunit 2 OS=Homo sapiens OX=9606 GN=ARPC2 PE=1 SV=1 |
| O15371 | EIF3D | Eukaryotic translation initiation factor 3 subunit D OS=Homo sapiens OX=9606 GN=EIF3D PE=1 SV=1 |
| O43795 | MYO1B | Unconventional myosin-Ib OS=Homo sapiens OX=9606 GN=MYO1B PE=1 SV=3 |
| O60244 | MED14 | Mediator of RNA polymerase II transcription subunit 14 OS=Homo sapiens OX=9606 GN=MED14 PE=1 SV=2 |
| O75592 | MYCBP2 | E3 ubiquitin-protein ligase MYCBP2 OS=Homo sapiens OX=9606 GN=MYCBP2 PE=1 SV=4 |
| O76015 | KRT38 | Keratin, type I cuticular Ha8 OS=Homo sapiens OX=9606 GN=KRT38 PE=1 SV=3 |
| O94826 | TOMM70 | Mitochondrial import receptor subunit TOM70 OS=Homo sapiens OX=9606 GN=TOMM70 PE=1 SV=1 |
| O94905 | ERLIN2 | Erlin-2 OS=Homo sapiens OX=9606 GN=ERLIN2 PE=1 SV=1 |
| O95071 | UBR5 | E3 ubiquitin-protein ligase UBR5 OS=Homo sapiens OX=9606 GN=UBR5 PE=1 SV=2 |
| O95163 | ELP1 | Elongator complex protein 1 OS=Homo sapiens OX=9606 GN=ELP1 PE=1 SV=3 |
| O95714 | HERC2 | E3 ubiquitin-protein ligase HERC2 OS=Homo sapiens OX=9606 GN=HERC2 PE=1 SV=2 |
| O95835 | LATS1 | Serine/threonine-protein kinase LATS1 OS=Homo sapiens OX=9606 GN=LATS1 PE=1 SV=1 |
| P00441 | SOD1 | Superoxide dismutase [Cu-Zn] OS=Homo sapiens OX=9606 GN=SOD1 PE=1 SV=2 |
| P00505 | GOT2 | Aspartate aminotransferase, mitochondrial OS=Homo sapiens OX=9606 GN=GOT2 PE=1 SV=3 |
| P00558 | PGK1 | Phosphoglycerate kinase 1 OS=Homo sapiens OX=9606 GN=PGK1 PE=1 SV=3 |
| P01860 | IGHG3 | Immunoglobulin heavy constant gamma 3 OS=Homo sapiens OX=9606 GN=IGHG3 PE=1 SV=2 |

| | | |
|---|---|---|
| P02461 | COL3A1 | Collagen alpha-1(III) chain OS=Homo sapiens OX=9606 GN=COL3A1 PE=1 SV=4 |
| P02656 | APOC3 | Apolipoprotein C-III OS=Homo sapiens OX=9606 GN=APOC3 PE=1 SV=1 |
| P02787 | TF | Serotransferrin OS=Homo sapiens OX=9606 GN=TF PE=1 SV=3 |
| P04279 | SEMG1 | Semenogelin-1 OS=Homo sapiens OX=9606 GN=SEMG1 PE=1 SV=2 |
| P05141 | SLC25A5 | ADP/ATP translocase 2 OS=Homo sapiens OX=9606 GN=SLC25A5 PE=1 SV=7 |
| P05164 | MPO | Myeloperoxidase OS=Homo sapiens OX=9606 GN=MPO PE=1 SV=1 |
| P05388 | RPLP0 | 60S acidic ribosomal protein P0 OS=Homo sapiens OX=9606 GN=RPLP0 PE=1 SV=1 |
| P06454 | PTMA | Prothymosin alpha OS=Homo sapiens OX=9606 GN=PTMA PE=1 SV=2 |
| P06703 | S100A6 | Protein S100-A6 OS=Homo sapiens OX=9606 GN=S100A6 PE=1 SV=1 |
| P06744 | GPI | Glucose-6-phosphate isomerase OS=Homo sapiens OX=9606 GN=GPI PE=1 SV=4 |
| P06748 | NPM1 | Nucleophosmin OS=Homo sapiens OX=9606 GN=NPM1 PE=1 SV=2 |
| P07305 | H1-0 | Histone H1.0 OS=Homo sapiens OX=9606 GN=H1-0 PE=1 SV=3 |
| P07477 | PRSS1 | Serine protease 1 OS=Homo sapiens OX=9606 GN=PRSS1 PE=1 SV=1 |
| P07910 | HNRNPC | Heterogeneous nuclear ribonucleoproteins C1/C2 OS=Homo sapiens OX=9606 GN=HNRNPC PE=1 SV=4 |
| P08246 | ELANE | Neutrophil elastase OS=Homo sapiens OX=9606 GN=ELANE PE=1 SV=1 |
| P08311 | CTSG | Cathepsin G OS=Homo sapiens OX=9606 GN=CTSG PE=1 SV=2 |
| P08758 | ANXA5 | Annexin A5 OS=Homo sapiens OX=9606 GN=ANXA5 PE=1 SV=2 |
| P09211 | GSTP1 | Glutathione S-transferase P OS=Homo sapiens OX=9606 GN=GSTP1 PE=1 SV=2 |
| P09622 | DLD | Dihydrolipoyl dehydrogenase, mitochondrial OS=Homo sapiens OX=9606 GN=DLD PE=1 SV=2 |
| P0DP04 | IGHV3-43D | Immunoglobulin heavy variable 3-43D OS=Homo sapiens OX=9606 GN=IGHV3-43D PE=3 SV=1 |
| P11387 | TOP1 | DNA topoisomerase 1 OS=Homo sapiens OX=9606 GN=TOP1 PE=1 SV=2 |
| P11940 | PABPC1 | Polyadenylate-binding protein 1 OS=Homo sapiens OX=9606 GN=PABPC1 PE=1 SV=2 |
| P12109 | COL6A1 | Collagen alpha-1(VI) chain OS=Homo sapiens OX=9606 GN=COL6A1 PE=1 SV=3 |
| P12111 | COL6A3 | Collagen alpha-3(VI) chain OS=Homo sapiens OX=9606 GN=COL6A3 PE=1 SV=5 |
| P12814 | ACTN1 | Alpha-actinin-1 OS=Homo sapiens OX=9606 GN=ACTN1 PE=1 SV=2 |

| | | |
|---|---|---|
| P16403 | H1-2 | Histone H1.2 OS=Homo sapiens OX=9606 GN=H1-2 PE=1 SV=2 |
| P16615 | ATP2A2 | Sarcoplasmic/endoplasmic reticulum calcium ATPase 2 OS=Homo sapiens OX=9606 GN=ATP2A2 PE=1 SV=1 |
| P17844 | DDX5 | Probable ATP-dependent RNA helicase DDX5 OS=Homo sapiens OX=9606 GN=DDX5 PE=1 SV=1 |
| P18077 | RPL35A | 60S ribosomal protein L35a OS=Homo sapiens OX=9606 GN=RPL35A PE=1 SV=2 |
| P18583 | SON | Protein SON OS=Homo sapiens OX=9606 GN=SON PE=1 SV=4 |
| P18621 | RPL17 | 60S ribosomal protein L17 OS=Homo sapiens OX=9606 GN=RPL17 PE=1 SV=3 |
| P19075 | TSPAN8 | Tetraspanin-8 OS=Homo sapiens OX=9606 GN=TSPAN8 PE=1 SV=1 |
| P21796 | VDAC1 | Voltage-dependent anion-selective channel protein 1 OS=Homo sapiens OX=9606 GN=VDAC1 PE=1 SV=2 |
| P22061 | PCMT1 | Protein-L-isoaspartate(D-aspartate) O-methyltransferase OS=Homo sapiens OX=9606 GN=PCMT1 PE=1 SV=4 |
| P22532 | SPRR2D | Small proline-rich protein 2D OS=Homo sapiens OX=9606 GN=SPRR2D PE=2 SV=2 |
| P23435 | CBLN1 | Cerebellin-1 OS=Homo sapiens OX=9606 GN=CBLN1 PE=1 SV=1 |
| P24278 | ZBTB25 | Zinc finger and BTB domain-containing protein 25 OS=Homo sapiens OX=9606 GN=ZBTB25 PE=1 SV=2 |
| P25786 | PSMA1 | Proteasome subunit alpha type-1 OS=Homo sapiens OX=9606 GN=PSMA1 PE=1 SV=1 |
| P25788 | PSMA3 | Proteasome subunit alpha type-3 OS=Homo sapiens OX=9606 GN=PSMA3 PE=1 SV=2 |
| P27105 | STOM | Stomatin OS=Homo sapiens OX=9606 GN=STOM PE=1 SV=3 |
| P30050 | RPL12 | 60S ribosomal protein L12 OS=Homo sapiens OX=9606 GN=RPL12 PE=1 SV=1 |
| P31930 | UQCRC1 | Cytochrome b-c1 complex subunit 1, mitochondrial OS=Homo sapiens OX=9606 GN=UQCRC1 PE=1 SV=3 |
| P35268 | RPL22 | 60S ribosomal protein L22 OS=Homo sapiens OX=9606 GN=RPL22 PE=1 SV=2 |
| P35914 | HMGCL | Hydroxymethylglutaryl-CoA lyase, mitochondrial OS=Homo sapiens OX=9606 GN=HMGCL PE=1 SV=2 |
| P42704 | LRPPRC | Leucine-rich PPR motif-containing protein, mitochondrial OS=Homo sapiens OX=9606 GN=LRPPRC PE=1 SV=3 |
| P46977 | STT3A | Dolichyl-diphosphooligosaccharide--protein glycosyltransferase subunit STT3A OS=Homo sapiens OX=9606 GN=STT3A PE=1 SV=2 |
| P47755 | CAPZA2 | F-actin-capping protein subunit alpha-2 OS=Homo sapiens OX=9606 GN=CAPZA2 PE=1 SV=3 |
| P47756 | CAPZB | F-actin-capping protein subunit beta OS=Homo sapiens OX=9606 GN=CAPZB PE=1 SV=5 |
| P47914 | RPL29 | 60S ribosomal protein L29 OS=Homo sapiens OX=9606 GN=RPL29 PE=1 SV=2 |
| P48047 | ATP5PO | ATP synthase subunit O, mitochondrial OS=Homo sapiens OX=9606 GN=ATP5PO PE=1 SV=1 |

| | | |
|---|---|---|
| P48594 | SERPINB4 | Serpin B4 OS=Homo sapiens OX=9606 GN=SERPINB4 PE=1 SV=2 |
| P49368 | CCT3 | T-complex protein 1 subunit gamma OS=Homo sapiens OX=9606 GN=CCT3 PE=1 SV=4 |
| P49411 | TUFM | Elongation factor Tu, mitochondrial OS=Homo sapiens OX=9606 GN=TUFM PE=1 SV=2 |
| P49750 | YLPM1 | YLP motif-containing protein 1 OS=Homo sapiens OX=9606 GN=YLPM1 PE=1 SV=4 |
| P50402 | EMD | Emerin OS=Homo sapiens OX=9606 GN=EMD PE=1 SV=1 |
| P50991 | CCT4 | T-complex protein 1 subunit delta OS=Homo sapiens OX=9606 GN=CCT4 PE=1 SV=4 |
| P51114 | FXR1 | RNA-binding protein FXR1 OS=Homo sapiens OX=9606 GN=FXR1 PE=1 SV=3 |
| P51148 | RAB5C | Ras-related protein Rab-5C OS=Homo sapiens OX=9606 GN=RAB5C PE=1 SV=2 |
| P51532 | SMARCA4 | Transcription activator BRG1 OS=Homo sapiens OX=9606 GN=SMARCA4 PE=1 SV=2 |
| P51572 | BCAP31 | B-cell receptor-associated protein 31 OS=Homo sapiens OX=9606 GN=BCAP31 PE=1 SV=3 |
| P51991 | HNRNPA3 | Heterogeneous nuclear ribonucleoprotein A3 OS=Homo sapiens OX=9606 GN=HNRNPA3 PE=1 SV=2 |
| P52907 | CAPZA1 | F-actin-capping protein subunit alpha-1 OS=Homo sapiens OX=9606 GN=CAPZA1 PE=1 SV=3 |
| P55060 | CSE1L | Exportin-2 OS=Homo sapiens OX=9606 GN=CSE1L PE=1 SV=3 |
| P55735 | SEC13 | Protein SEC13 homolog OS=Homo sapiens OX=9606 GN=SEC13 PE=1 SV=3 |
| P61158 | ACTR3 | Actin-related protein 3 OS=Homo sapiens OX=9606 GN=ACTR3 PE=1 SV=3 |
| P61160 | ACTR2 | Actin-related protein 2 OS=Homo sapiens OX=9606 GN=ACTR2 PE=1 SV=1 |
| P62244 | RPS15A | 40S ribosomal protein S15a OS=Homo sapiens OX=9606 GN=RPS15A PE=1 SV=2 |
| P62266 | RPS23 | 40S ribosomal protein S23 OS=Homo sapiens OX=9606 GN=RPS23 PE=1 SV=3 |
| P62277 | RPS13 | 40S ribosomal protein S13 OS=Homo sapiens OX=9606 GN=RPS13 PE=1 SV=2 |
| P62424 | RPL7A | 60S ribosomal protein L7a OS=Homo sapiens OX=9606 GN=RPL7A PE=1 SV=2 |
| P62701 | RPS4X | 40S ribosomal protein S4, X isoform OS=Homo sapiens OX=9606 GN=RPS4X PE=1 SV=2 |
| P62750 | RPL23A | 60S ribosomal protein L23a OS=Homo sapiens OX=9606 GN=RPL23A PE=1 SV=1 |
| P62753 | RPS6 | 40S ribosomal protein S6 OS=Homo sapiens OX=9606 GN=RPS6 PE=1 SV=1 |
| P62847 | RPS24 | 40S ribosomal protein S24 OS=Homo sapiens OX=9606 GN=RPS24 PE=1 SV=1 |
| P62861 | FAU | FAU ubiquitin-like and ribosomal protein S30 OS=Homo sapiens OX=9606 GN=FAU PE=1 SV=2 |

| | | |
|---|---|---|
| P62873 | GNB1 | Guanine nucleotide-binding protein G(I)/G(S)/G(T) subunit beta-1 OS=Homo sapiens OX=9606 GN=GNB1 PE=1 SV=3 |
| P62917 | RPL8 | 60S ribosomal protein L8 OS=Homo sapiens OX=9606 GN=RPL8 PE=1 SV=2 |
| P62995 | TRA2B | Transformer-2 protein homolog beta OS=Homo sapiens OX=9606 GN=TRA2B PE=1 SV=1 |
| P63104 | YWHAZ | 14-3-3 protein zeta/delta OS=Homo sapiens OX=9606 GN=YWHAZ PE=1 SV=1 |
| P63244 | RACK1 | Receptor of activated protein C kinase 1 OS=Homo sapiens OX=9606 GN=RACK1 PE=1 SV=3 |
| P67809 | YBX1 | Y-box-binding protein 1 OS=Homo sapiens OX=9606 GN=YBX1 PE=1 SV=3 |
| P78371 | CCT2 | T-complex protein 1 subunit beta OS=Homo sapiens OX=9606 GN=CCT2 PE=1 SV=4 |
| P82094 | TMF1 | TATA element modulatory factor OS=Homo sapiens OX=9606 GN=TMF1 PE=1 SV=2 |
| P83881 | RPL36A | 60S ribosomal protein L36a OS=Homo sapiens OX=9606 GN=RPL36A PE=1 SV=2 |
| Q00610 | CLTC | Clathrin heavy chain 1 OS=Homo sapiens OX=9606 GN=CLTC PE=1 SV=5 |
| Q01081 | U2AF1 | Splicing factor U2AF 35 kDa subunit OS=Homo sapiens OX=9606 GN=U2AF1 PE=1 SV=3 |
| Q02383 | SEMG2 | Semenogelin-2 OS=Homo sapiens OX=9606 GN=SEMG2 PE=1 SV=1 |
| Q04637 | EIF4G1 | Eukaryotic translation initiation factor 4 gamma 1 OS=Homo sapiens OX=9606 GN=EIF4G1 PE=1 SV=4 |
| Q05639 | EEF1A2 | Elongation factor 1-alpha 2 OS=Homo sapiens OX=9606 GN=EEF1A2 PE=1 SV=1 |
| Q07666 | KHDRBS1 | KH domain-containing, RNA-binding, signal transduction-associated protein 1 OS=Homo sapiens OX=9606 GN=KHDRBS1 PE=1 SV=1 |
| Q08379 | GOLGA2 | Golgin subfamily A member 2 OS=Homo sapiens OX=9606 GN=GOLGA2 PE=1 SV=3 |
| Q10570 | CPSF1 | Cleavage and polyadenylation specificity factor subunit 1 OS=Homo sapiens OX=9606 GN=CPSF1 PE=1 SV=2 |
| Q13085 | ACACA | Acetyl-CoA carboxylase 1 OS=Homo sapiens OX=9606 GN=ACACA PE=1 SV=2 |
| Q13185 | CBX3 | Chromobox protein homolog 3 OS=Homo sapiens OX=9606 GN=CBX3 PE=1 SV=4 |
| Q13310 | PABPC4 | Polyadenylate-binding protein 4 OS=Homo sapiens OX=9606 GN=PABPC4 PE=1 SV=1 |
| Q13510 | ASAH1 | Acid ceramidase OS=Homo sapiens OX=9606 GN=ASAH1 PE=1 SV=5 |
| Q13885 | TUBB2A | Tubulin beta-2A chain OS=Homo sapiens OX=9606 GN=TUBB2A PE=1 SV=1 |
| Q14498 | RBM39 | RNA-binding protein 39 OS=Homo sapiens OX=9606 GN=RBM39 PE=1 SV=2 |
| Q14533 | KRT81 | Keratin, type II cuticular Hb1 OS=Homo sapiens OX=9606 GN=KRT81 PE=1 SV=3 |

| | | |
|---|---|---|
| Q14686 | NCOA6 | Nuclear receptor coactivator 6 OS=Homo sapiens OX=9606 GN=NCOA6 PE=1 SV=3 |
| Q14974 | KPNB1 | Importin subunit beta-1 OS=Homo sapiens OX=9606 GN=KPNB1 PE=1 SV=2 |
| Q14980 | NUMA1 | Nuclear mitotic apparatus protein 1 OS=Homo sapiens OX=9606 GN=NUMA1 PE=1 SV=2 |
| Q15029 | EFTUD2 | 116 kDa U5 small nuclear ribonucleoprotein component OS=Homo sapiens OX=9606 GN=EFTUD2 PE=1 SV=1 |
| Q15233 | NONO | Non-POU domain-containing octamer-binding protein OS=Homo sapiens OX=9606 GN=NONO PE=1 SV=4 |
| Q15424 | SAFB | Scaffold attachment factor B1 OS=Homo sapiens OX=9606 GN=SAFB PE=1 SV=4 |
| Q15436 | SEC23A | Protein transport protein Sec23A OS=Homo sapiens OX=9606 GN=SEC23A PE=1 SV=2 |
| Q15582 | TGFBI | Transforming growth factor-beta-induced protein ig-h3 OS=Homo sapiens OX=9606 GN=TGFBI PE=1 SV=1 |
| Q15637 | SF1 | Splicing factor 1 OS=Homo sapiens OX=9606 GN=SF1 PE=1 SV=4 |
| Q15911 | ZFHX3 | Zinc finger homeobox protein 3 OS=Homo sapiens OX=9606 GN=ZFHX3 PE=1 SV=2 |
| Q16658 | FSCN1 | Fascin OS=Homo sapiens OX=9606 GN=FSCN1 PE=1 SV=3 |
| Q16778 | H2BC21 | Histone H2B type 2-E OS=Homo sapiens OX=9606 GN=H2BC21 PE=1 SV=3 |
| Q5T481 | RBM20 | RNA-binding protein 20 OS=Homo sapiens OX=9606 GN=RBM20 PE=1 SV=4 |
| Q5T4S7 | UBR4 | E3 ubiquitin-protein ligase UBR4 OS=Homo sapiens OX=9606 GN=UBR4 PE=1 SV=1 |
| Q63HN8 | RNF213 | E3 ubiquitin-protein ligase RNF213 OS=Homo sapiens OX=9606 GN=RNF213 PE=1 SV=3 |
| Q6E0U4 | DMKN | Dermokine OS=Homo sapiens OX=9606 GN=DMKN PE=1 SV=3 |
| Q6GMR7 | FAAH2 | Fatty-acid amide hydrolase 2 OS=Homo sapiens OX=9606 GN=FAAH2 PE=1 SV=1 |
| Q6NZI2 | CAVIN1 | Caveolae-associated protein 1 OS=Homo sapiens OX=9606 GN=CAVIN1 PE=1 SV=1 |
| Q6ZVX7 | NCCRP1 | F-box only protein 50 OS=Homo sapiens OX=9606 GN=NCCRP1 PE=1 SV=1 |
| Q7Z3Y8 | KRT27 | Keratin, type I cytoskeletal 27 OS=Homo sapiens OX=9606 GN=KRT27 PE=1 SV=2 |
| Q7Z417 | NUFIP2 | FMR1-interacting protein NUFIP2 OS=Homo sapiens OX=9606 GN=NUFIP2 PE=1 SV=1 |
| Q7Z6Z7 | HUWE1 | E3 ubiquitin-protein ligase HUWE1 OS=Homo sapiens OX=9606 GN=HUWE1 PE=1 SV=3 |
| Q86T82 | USP37 | Ubiquitin carboxyl-terminal hydrolase 37 OS=Homo sapiens OX=9606 GN=USP37 PE=1 SV=2 |
| Q8IUD2 | ERC1 | ELKS/Rab6-interacting/CAST family member 1 OS=Homo sapiens OX=9606 GN=ERC1 PE=1 SV=1 |
| Q8IW75 | SERPINA12 | Serpin A12 OS=Homo sapiens OX=9606 GN=SERPINA12 PE=1 SV=1 |

| | | |
|---|---|---|
| Q8IWA0 | WDR75 | WD repeat-containing protein 75 OS=Homo sapiens OX=9606 GN=WDR75 PE=1 SV=1 |
| Q8IYB3 | SRRM1 | Serine/arginine repetitive matrix protein 1 OS=Homo sapiens OX=9606 GN=SRRM1 PE=1 SV=2 |
| Q8N3X1 | FNBP4 | Formin-binding protein 4 OS=Homo sapiens OX=9606 GN=FNBP4 PE=1 SV=3 |
| Q8NC51 | SERBP1 | Plasminogen activator inhibitor 1 RNA-binding protein OS=Homo sapiens OX=9606 GN=SERBP1 PE=1 SV=2 |
| Q8NCA5 | FAM98A | Protein FAM98A OS=Homo sapiens OX=9606 GN=FAM98A PE=1 SV=2 |
| Q8ND56 | LSM14A | Protein LSM14 homolog A OS=Homo sapiens OX=9606 GN=LSM14A PE=1 SV=3 |
| Q8NEX9 | SDR9C7 | Short-chain dehydrogenase/reductase family 9C member 7 OS=Homo sapiens OX=9606 GN=SDR9C7 PE=1 SV=1 |
| Q8NEZ4 | KMT2C | Histone-lysine N-methyltransferase 2C OS=Homo sapiens OX=9606 GN=KMT2C PE=1 SV=3 |
| Q8NI35 | PATJ | InaD-like protein OS=Homo sapiens OX=9606 GN=PATJ PE=1 SV=3 |
| Q8WWM7 | ATXN2L | Ataxin-2-like protein OS=Homo sapiens OX=9606 GN=ATXN2L PE=1 SV=2 |
| Q8WXX0 | DNAH7 | Dynein axonemal heavy chain 7 OS=Homo sapiens OX=9606 GN=DNAH7 PE=1 SV=2 |
| Q92616 | GCN1 | eIF-2-alpha kinase activator GCN1 OS=Homo sapiens OX=9606 GN=GCN1 PE=1 SV=7 |
| Q92794 | KAT6A | Histone acetyltransferase KAT6A OS=Homo sapiens OX=9606 GN=KAT6A PE=1 SV=2 |
| Q92900 | UPF1 | Regulator of nonsense transcripts 1 OS=Homo sapiens OX=9606 GN=UPF1 PE=1 SV=2 |
| Q93074 | MED12 | Mediator of RNA polymerase II transcription subunit 12 OS=Homo sapiens OX=9606 GN=MED12 PE=1 SV=4 |
| Q96CW1 | AP2M1 | AP-2 complex subunit mu OS=Homo sapiens OX=9606 GN=AP2M1 PE=1 SV=2 |
| Q96EK7 | FAM120B | Constitutive coactivator of peroxisome proliferator-activated receptor gamma OS=Homo sapiens OX=9606 GN=FAM120B PE=1 SV=1 |
| Q96IZ0 | PAWR | PRKC apoptosis WT1 regulator protein OS=Homo sapiens OX=9606 GN=PAWR PE=1 SV=1 |
| Q96JH8 | RADIL | Ras-associating and dilute domain-containing protein OS=Homo sapiens OX=9606 GN=RADIL PE=1 SV=5 |
| Q96N67 | DOCK7 | Dedicator of cytokinesis protein 7 OS=Homo sapiens OX=9606 GN=DOCK7 PE=1 SV=4 |
| Q99578 | RIT2 | GTP-binding protein Rit2 OS=Homo sapiens OX=9606 GN=RIT2 PE=1 SV=1 |
| Q99848 | EBNA1BP2 | Probable rRNA-processing protein EBP2 OS=Homo sapiens OX=9606 GN=EBNA1BP2 PE=1 SV=2 |
| Q9BQG0 | MYBBP1A | Myb-binding protein 1A OS=Homo sapiens OX=9606 GN=MYBBP1A PE=1 SV=2 |
| Q9BRL6 | SRSF8 | Serine/arginine-rich splicing factor 8 OS=Homo sapiens OX=9606 GN=SRSF8 PE=1 SV=1 |

| | | |
|---|---|---|
| Q9C0H5 | ARHGAP39 | Rho GTPase-activating protein 39 OS=Homo sapiens OX=9606 GN=ARHGAP39 PE=1 SV=2 |
| Q9H0U3 | MAGT1 | Magnesium transporter protein 1 OS=Homo sapiens OX=9606 GN=MAGT1 PE=1 SV=1 |
| Q9H1E1 | RNASE7 | Ribonuclease 7 OS=Homo sapiens OX=9606 GN=RNASE7 PE=1 SV=2 |
| Q9H307 | PNN | Pinin OS=Homo sapiens OX=9606 GN=PNN PE=1 SV=5 |
| Q9H583 | HEATR1 | HEAT repeat-containing protein 1 OS=Homo sapiens OX=9606 GN=HEATR1 PE=1 SV=3 |
| Q9H6D7 | HAUS4 | HAUS augmin-like complex subunit 4 OS=Homo sapiens OX=9606 GN=HAUS4 PE=1 SV=1 |
| Q9HC35 | EML4 | Echinoderm microtubule-associated protein-like 4 OS=Homo sapiens OX=9606 GN=EML4 PE=1 SV=3 |
| Q9HCE1 | MOV10 | Helicase MOV-10 OS=Homo sapiens OX=9606 GN=MOV10 PE=1 SV=2 |
| Q9NQ29 | LUC7L | Putative RNA-binding protein Luc7-like 1 OS=Homo sapiens OX=9606 GN=LUC7L PE=1 SV=1 |
| Q9NR30 | DDX21 | Nucleolar RNA helicase 2 OS=Homo sapiens OX=9606 GN=DDX21 PE=1 SV=5 |
| Q9NTK1 | DEPP1 | Protein DEPP1 OS=Homo sapiens OX=9606 GN=DEPP1 PE=1 SV=2 |
| Q9NU22 | MDN1 | Midasin OS=Homo sapiens OX=9606 GN=MDN1 PE=1 SV=2 |
| Q9NUG4 | CCM2L | Cerebral cavernous malformations 2 protein-like OS=Homo sapiens OX=9606 GN=CCM2L PE=1 SV=3 |
| Q9NZ01 | TECR | Very-long-chain enoyl-CoA reductase OS=Homo sapiens OX=9606 GN=TECR PE=1 SV=1 |
| Q9NZB2 | FAM120A | Constitutive coactivator of PPAR-gamma-like protein 1 OS=Homo sapiens OX=9606 GN=FAM120A PE=1 SV=2 |
| Q9NZD8 | SPG21 | Maspardin OS=Homo sapiens OX=9606 GN=SPG21 PE=1 SV=1 |
| Q9NZI8 | IGF2BP1 | Insulin-like growth factor 2 mRNA-binding protein 1 OS=Homo sapiens OX=9606 GN=IGF2BP1 PE=1 SV=2 |
| Q9P219 | CCDC88C | Protein Daple OS=Homo sapiens OX=9606 GN=CCDC88C PE=1 SV=3 |
| Q9P2I0 | CPSF2 | Cleavage and polyadenylation specificity factor subunit 2 OS=Homo sapiens OX=9606 GN=CPSF2 PE=1 SV=2 |
| Q9UBG3 | CRNN | Cornulin OS=Homo sapiens OX=9606 GN=CRNN PE=1 SV=1 |
| Q9UBM7 | DHCR7 | 7-dehydrocholesterol reductase OS=Homo sapiens OX=9606 GN=DHCR7 PE=1 SV=1 |
| Q9ULX6 | AKAP8L | A-kinase anchor protein 8-like OS=Homo sapiens OX=9606 GN=AKAP8L PE=1 SV=4 |
| Q9UN86 | G3BP2 | Ras GTPase-activating protein-binding protein 2 OS=Homo sapiens OX=9606 GN=G3BP2 PE=1 SV=2 |
| Q9UQ35 | SRRM2 | Serine/arginine repetitive matrix protein 2 OS=Homo sapiens OX=9606 GN=SRRM2 PE=1 SV=2 |
| Q9Y2W1 | THRAP3 | Thyroid hormone receptor-associated protein 3 OS=Homo sapiens OX=9606 GN=THRAP3 PE=1 SV=2 |
| Q9Y3R4 | NEU2 | Sialidase-2 OS=Homo sapiens OX=9606 GN=NEU2 PE=1 SV=2 |
| Q9Y4L1 | HYOU1 | Hypoxia up-regulated protein 1 OS=Homo sapiens OX=9606 GN=HYOU1 PE=1 SV=1 |

| | | |
|---|---|---|
| Q9Y5B9 | SUPT16H | FACT complex subunit SPT16 OS=Homo sapiens OX=9606 GN=SUPT16H PE=1 SV=1 |

**Supplementary Table 12. Protein with enhanced binding to FBXO7 in degenerated NP cells.**

| Accession | GeneName | Description |
|---|---|---|
| Q93074 | MED12 | Mediator of RNA polymerase II transcription subunit 12 OS=Homo sapiens OX=9606 GN=MED12 PE=1 SV=4 |
| Q9UKV3 | ACIN1 | Apoptotic chromatin condensation inducer in the nucleus OS=Homo sapiens OX=9606 GN=ACIN1 PE=1 SV=2 |
| P16403 | H1-2 | Histone H1.2 OS=Homo sapiens OX=9606 GN=H1-2 PE=1 SV=2 |
| Q15436 | SEC23A | Protein transport protein Sec23A OS=Homo sapiens OX=9606 GN=SEC23A PE=1 SV=2 |
| Q5UIP0 | RIF1 | Telomere-associated protein RIF1 OS=Homo sapiens OX=9606 GN=RIF1 PE=1 SV=2 |
| Q9Y2W1 | THRAP3 | Thyroid hormone receptor-associated protein 3 OS=Homo sapiens OX=9606 GN=THRAP3 PE=1 SV=2 |
| Q8NHV4 | NEDD1 | Protein NEDD1 OS=Homo sapiens OX=9606 GN=NEDD1 PE=1 SV=1 |
| P47914 | RPL29 | Large ribosomal subunit protein eL29 OS=Homo sapiens OX=9606 GN=RPL29 PE=1 SV=2 |
| A0A2R8Y4L2 | HNRNPA1L3 | Heterogeneous nuclear ribonucleoprotein A1-like 3 OS=Homo sapiens OX=9606 GN=HNRNPA1L3 PE=1 SV=2 |
| P48634 | PRRC2A | Protein PRRC2A OS=Homo sapiens OX=9606 GN=PRRC2A PE=1 SV=3 |
| Q99878 | H2AC14 | Histone H2A type 1-J OS=Homo sapiens OX=9606 GN=H2AC14 PE=1 SV=3 |
| Q9ULJ3 | ZBTB21 | Zinc finger and BTB domain-containing protein 21 OS=Homo sapiens OX=9606 GN=ZBTB21 PE=1 SV=2 |
| Q29980 | MICB | MHC class I polypeptide-related sequence B OS=Homo sapiens OX=9606 GN=MICB PE=1 SV=2 |
| Q16629 | SRSF7 | Serine/arginine-rich splicing factor 7 OS=Homo sapiens OX=9606 GN=SRSF7 PE=1 SV=1 |
| Q15437 | SEC23B | Protein transport protein Sec23B OS=Homo sapiens OX=9606 GN=SEC23B PE=1 SV=2 |

| | | |
|---|---|---|
| O00425 | IGF2BP3 | Insulin-like growth factor 2 mRNA-binding protein 3 OS=Homo sapiens OX=9606 GN=IGF2BP3 PE=1 SV=2 |
| Q9Y3Y2 | CHTOP | Chromatin target of PRMT1 protein OS=Homo sapiens OX=9606 GN=CHTOP PE=1 SV=2 |
| P62851 | RPS25 | Small ribosomal subunit protein eS25 OS=Homo sapiens OX=9606 GN=RPS25 PE=1 SV=1 |
| P62995 | TRA2B | Transformer-2 protein homolog beta OS=Homo sapiens OX=9606 GN=TRA2B PE=1 SV=1 |
| P84098 | RPL19 | Large ribosomal subunit protein eL19 OS=Homo sapiens OX=9606 GN=RPL19 PE=1 SV=1 |
| Q86U42 | PABPN1 | Polyadenylate-binding protein 2 OS=Homo sapiens OX=9606 GN=PABPN1 PE=1 SV=3 |
| Q14839 | CHD4 | Chromodomain-helicase-DNA-binding protein 4 OS=Homo sapiens OX=9606 GN=CHD4 PE=1 SV=2 |
| Q14980 | NUMA1 | Nuclear mitotic apparatus protein 1 OS=Homo sapiens OX=9606 GN=NUMA1 PE=1 SV=2 |
| P10809 | HSPD1 | 60 kDa heat shock protein, mitochondrial OS=Homo sapiens OX=9606 GN=HSPD1 PE=1 SV=2 |
| Q8IX01 | SUGP2 | SURP and G-patch domain-containing protein 2 OS=Homo sapiens OX=9606 GN=SUGP2 PE=1 SV=2 |
| Q8NI36 | WDR36 | WD repeat-containing protein 36 OS=Homo sapiens OX=9606 GN=WDR36 PE=1 SV=1 |
| Q9BPU6 | DPYSL5 | Dihydropyrimidinase-related protein 5 OS=Homo sapiens OX=9606 GN=DPYSL5 PE=1 SV=1 |
| Q5TEC6 | H3-7 | Histone H3-7 OS=Homo sapiens OX=9606 GN=H3-7 PE=1 SV=1 |
| Q9Y623 | MYH4 | Myosin-4 OS=Homo sapiens OX=9606 GN=MYH4 PE=1 SV=2 |
| A4UGR9 | XIRP2 | Xin actin-binding repeat-containing protein 2 OS=Homo sapiens OX=9606 GN=XIRP2 PE=1 SV=2 |